APPLYING EVS-ENCAPSULATED CRISPR RIBONUCLEOPROTEIN COMPLEX FOR

GENE EDITING IN VIVO

Bv

DEBASHISH MONDOL

(Under the Direction of Houjian Cai)

ABSTRACT

The safe and efficient delivery of CRISPR/Cas9 remains a major challenge in advancing clinical

gene-editing applications. This study investigates the use of extracellular vesicles (EVs) coated

with VSV-G for CRISPR/Cas9 ribonucleoprotein complexes targeting the eGFP gene. HEK293T

cells were engineered to produce EVs co-expressing mCas9/sgRNA and VSV-G. The isolated EVs

achieved 14.67% ±7.02 gene editing efficiency in HEK293T-eGFP cells. Notably, compared with

VSV-G, SARS-CoV-2 spike(D614G-Δ21) protein inhibited the encapsulation of mCas9/sgRNA

into EVs. SCID mice expressing EGFP or carrying EGFP xenograft tissues were administered EVs

co-expressing VSV-G and mCas9/sgRNA targeting the eGFP gene by intravenous injection. No

observable weight loss was detected, suggesting their safety and biocompatibility. Next-generation

sequencing revealed 2% insertions and deletions in lung tissue and 1% in xenograft tissues. These

results highlight EVs expressing VSV-G, but not spike protein, as an effective approach for

CRISPR/Cas9 delivery; however, the delivery route needs further optimization of gene-editing

efficiency in vivo.

INDEX WORDS: Extracellular vesicles, CRISPR/Cas9, VSV-G, Xenograft tumor

APPLYING EVS-ENCAPSULATED CRISPR RIBONUCLEOPROTEIN COMPLEX FOR GENE EDITING IN VIVO

By

DEBASHISH MONDOL

BS, Jashore University of Science and Technology, Bangladesh, 2017

A Thesis Submitted to the Graduate Faculty of The University of Georgia in Partial Fulfillment of the Requirements for the Degree

MASTER OF SCIENCE

ATHENS, GEORGIA

2025

© 2025

Debashish Mondol

All Rights Reserved

APPLYING EVS-ENCAPSULATED CRISPR RIBONUCLEOPROTEIN COMPLEX FOR GENE EDITING IN VIVO

By

DEBASHISH MONDOL

Major Professor: Houjian Cai Wendy Watford Committee: Bin Yi

Electronic Version Approved:

Ron Walcott Vice Provost for Graduate Education and Dean of the Graduate School The University of Georgia August 2025

DEDICATION

My thesis is dedicated to my family. My heartfelt appreciation goes out to my parents, Bhudeb Chandra Mondol and Latika Mondol. Their unconditional love, sacrifices, and unwavering support have been the cornerstone of my journey. Their strength and guidance have inspired in me perseverance, resilience, and a deep appreciation for the value of hard work.

I am endlessly grateful to my wife, Sonchita Biswas. Her constant support, understanding, and patience have been my greatest strength throughout this journey. Her love, companionship, and faith in my potential have been my anchor and motivation. This achievement would not have been possible without her presence in my life.

I also dedicate this work to the cherished memory of my beloved youngest sister,

Champa Mondol. Though she is no longer by my side, her love, laughter, and spirit continue to

live within me, guiding my steps and inspiring me every day. Her memory is a constant reminder

of resilience, hope, and the strength to carry on.

Additionally, I dedicate my thesis to my numerous friends and my whole family. I will always be grateful for everything they have done. They consistently show me concern, which makes me feel warm within.

ACKNOWLEDGEMENTS

I would like to thank my committee members, who were exceedingly kind with their knowledge and time. Dr. Houjian Cai, my PI, deserves special recognition for his endless hours of thoughtful mentorship, critical feedback, encouragement, and most importantly, patience during the whole program. Drs. Wendy Watford and Bin Yi, I sincerely appreciate your willingness to serve on my committee and for providing me extremely useful advice and thoughtful input that greatly enriched my project.

I am so grateful for everyone in our lab, Drs. Joseph Andrew Whitley and Chenming Ye, Ms. Jennifer Lathrop, and Mr. Dawei Zong, for their guidance and hands-on help during my experiments. I would like to appreciate and thank College of Pharmacy for granting me chances and offering support. Special appreciation is extended to the Graduate school and human resources departments for their assistance.

Lastly, I would want to thank all the faculties and staff who aided me with my project. Your enthusiasm and warm heart to offer help made this research project a pleasure to do.

This work was supported by the NIH under U01 CA225784-01; R21AI157831-01A1; The American Institute for Cancer Research.

TABLE OF CONTENTS

	Page
ACKNO	OWLEDGEMENTS
TABLE	OF CONTENTSv
LIST OF	F FIGURESix
INTROI	DUCTION1
1. (Clustered Regularly Interspaced Short Palindromic Repeats (CRISPR)-Associated
Protei	n 9 (Cas9) System
2. (CRISPR-Cas9 System Delivery Methods6
3. (Carriers for Delivering CRISPR Technology6
4. I	Limitations of Targeted Delivery
5. I	Extracellular Vesicles (EVs) to Deliver CRISPR/Cas9
6. I	Extracellular Vesicles Delivery
7. (CRISPR/Cas9 Delivery via EVs19
EXPER!	IMENTAL METHODS21
1. (Cell Culture
2. I	Plasmids Preparation
3. I	Protein Extraction and Western Blotting
4. F	Polymerase Chain Reaction (PCR) and DNA Sequencing23

	5.	T7 Endonuclease Assay	24
	6.	Production and Isolation of EVs Encapsulating mCas9/sgRNA-eGFP and Coated with	
	VSV	V-G and/or Spike(D614G- Δ 21)	25
	7.	EVs Characterization and Size Distribution	25
	8.	EVs Mediated Genome Editing in HEK293T-eGFP Cells	26
	9.	In Vivo Endogenous eGFP Gene Editing in Various Organs of NOD-SCID-EGFP Mou	ise
	Usir	ng EV-Encapsulated CRISPR/Cas9 RNPs	26
	10.	In Vivo eGFP Gene Editing in Xenograft Tissues in NOD-SCID-EGFP Mouse Using	or S
	EVs	Encapsulated CRISPR/Cas9 RNPs	28
	11.	Statistical Analysis	28
R	ESU	LTS	30
	1.	mCas9/sgRNA Plasmid Targeting the eGFP Gene Induced Efficient Gene Editing in	
	HEI	K293T-eGFP Cells	30
	2.	Isolation and characterization of EVs and confirmation of VSV-G and mCas9 expression	on
	in th	ne EVs	31
	3.	EVs Coated with VSV-G and Encapsulating mCas9/sgRNA Knocked out the eGFP Ge	ene
	in H	EK293T-eGFP Cells	34
	4.	Spike Viral Protein Inhibited EVs Production and mCas9 Encapsulation Efficiency	37
	5.	In Vivo Evaluation of Endogenous eGFP Gene Editing in Various Organs Using EVs	
	Enc	apsulating mCas9/sgRNA RNPs in NOD-SCID-EGFP Mouse Models	40

6.	In Vivo Evaluation of eGFP Gene Editing in Xenograft Tissues Using EVs Encapsulating	ıg
mС	Cas9/sgRNA RNPs in NOD-SCID-EGFP Mouse Models	43
DISC	USSION	46
1.	CRISPR/Cas9-Mediated Gene Editing Efficiency in HEK293T-eGFP Cells	47
2.	Production and Characterization of VSV-G Coated EVs Encapsulating mCas9/sgRNA	47
3.	Genome Editing Activity of EVs-Delivered CRISPR RNPs in HEK293T-eGFP Cells4	48
4.	Spike(D614G-Δ21) Inhibits the EVs Biogenesis and Cas9 Encapsulation Efficiency	
Coı	mpared with VSV-G	49
5.	Systemic Delivery of CRISPR RNP Loaded EVs Demonstrates In Vivo Genome Editing	3
	51	
LIMI	TATIONS AND FUTURE DIRECTIONS	55
CON	CLUSION	56
DEEE	PENCES 4	5

LIST OF FIGURES

Page
Figure 1 Mechanism and cellular delivery of CRISPR–Cas9 gene editing system 5
Figure 2 Overview of various delivery vectors used for <i>in vivo</i> CRISPR system administration 9
Figure 3 Overview of EVs biogenesis and cellular uptake mechanisms
Figure 4 eGFP gene knockout in HEK293T-eGFP cells using mCas9/sgRNA plasmid 31
Figure 5 Production and characterization of EVs coated with VSV-G and encapsulating
mCas9/sgRNA
Figure 6 EVs encapsulating mCas9/sgRNA RNP complex coated with VSV-G mediated eGFP
gene knockout in HEK293T-eGFP cells
Figure 7 Spike(D614G-Δ21) viral membrane protein inhibited EVs production and mCas9
encapsulation efficiency compared to VSV-G
Figure 8 In vivo genome editing using EVs encapsulating mCas9/sgRNA-eGFP RNPs and coated
with VSV-G in NSG-EGFP mouse models. 42
Figure 9 In vivo genome editing in xenograft tissues using EVs encapsulating mCas9/sgRNA-
eGFP RNPs and coated with VSV-G in SCID mouse model

CHAPTER 1

INTRODUCTION

Genome editing has emerged as a transformative technology that allows for precise modification in the genomic sequence through insertions, deletions, or substitution of specific DNA sequences. This approach holds particular promise for treating a range of diseases, especially genetic disorders and cancers linked to single-gene mutations, aiming to introduce targeted changes into cellular DNA using its own repair mechanisms. While various delivery methods have been explored, including physical techniques, viral vectors such as lentiviruses or adeno-associated viruses (AAV), and non-viral carriers like lipid-based systems and nanoparticles, these approaches still face considerable limitations. EVs have emerged as a highly promising alternative for delivering CRISPR/Cas9 components, effectively overcoming many of the limitations posed by traditional delivery systems. Due to their modifiability, low immunogenicity, and efficient uptake, EVs are considered a safe and practical option for delivering a wide array of therapeutic molecules^{4,5}. In this study we have studied EVs as the delivery system for CRISPR machinery to target the eGFP gene in both *in vitro* and *in vivo* models.

1. Clustered Regularly Interspaced Short Palindromic Repeats (CRISPR)-Associated Protein 9 (Cas9) System

The CRISPR/Cas9 system is a greatly promising cutting-edge technology for advancing gene therapy. The CRISPR/Cas9 system was originally identified as part of a bacterial adaptive immune response to viral infections ^{6,7} and has been reengineered into a highly effective RNA-guided genome editing platform.

Discovery of CRISPR/Cas9 system. The origins of the CRISPR-Cas9 system trace back to 1987 when a team of Japanese researchers led by Ishino et al. discovered an unusual repetitive DNA sequence at the 3' end of the iap gene in *Escherichia coli*. This sequence consisted of five nearly identical repeats, each 29 nucleotides long and separated by unique 32-nucleotide sequences. 8 The biological significance of these clustered repeats remained unclear until 1995, when Spanish molecular biologist Francisco Mojica identified similar sequences in the archeal genome of Haloferax mediterranei, despite having the challenges in sequencing at that time⁷. Mojica proposed that these DNA repeats might be part of the bacteria and archaea immune system⁹. In 2002, the acronym CRISPR—short for Clustered Regularly Interspaced Short Palindromic Repeats—was introduced by Jansen and colleagues, 10 who also noted the presence of CRISPR-associated (Cas) genes, including Cas1 to Cas4. In 2005, researchers discovered that the spacers between the palindromic repeats (ranging from 17 to 84 bases) were fragments of viral DNA, while the repeats themselves (typically 23 to 50 bases)¹¹ were palindromic in nature and likely derived from bacteriophages^{6,12}. In 2007, scientists demonstrated that these viral DNA fragments were acquired and stored at CRISPR loci, enabling bacteria to mount adaptive immune responses against phage infections¹³. John van der Oost's group at Wageningen University in 2008 discovered that these loci are transcribed into CRISPR RNAs (crRNAs), which contain the spacer and repeat sequences¹⁴. Then in 2011, Emmanuelle Charpentier's team identified another RNA component, known as trans-activating CRISPR RNA (tracrRNA), essential for the maturation and function of crRNAs¹⁵. This discovery ultimately led to the development of a simplified single-guide RNA (sgRNA), created by fusing crRNA and tracrRNA, dramatically improving the efficiency and applicability of the CRISPR-Cas9 system in *in vitro* research¹⁶ that work led to a Nobel Prize.

Based on genetic and structural differences, CRISPR-Cas systems are divided into two classes, and Cas9, the most widely studied and utilized enzyme, belongs to Class II^{17,18}. While Class I systems rely on large multi-protein complexes to cleave DNA, Class II systems like Cas9 achieve this with a single effector protein. In 2013, researchers including Cong and Mali demonstrated the successful use of the Type II CRISPR-Cas system for targeted gene editing in mammalian cells^{19,20}. This achievement opened the door for the application of CRISPR-Cas9 system in genome modification.

Mechanisms of CRISPR-Cas9 system. Many bacteria and the majority of archaea have developed advanced RNA-guided adaptive immune systems encoded by CRISPR loci and associated Cas genes, to defend against bacteriophage attacks and plasmid-mediated gene transfer^{21–23}. These CRISPR systems work by integrating short sequences of foreign DNA, known as protospacers, from invading bacteria into the CRISPR locus²⁴. Following integration, these protospacer sequences are transcribed and enzymatically processed into short mature CRISPR RNAs (crRNAs), which form complexes with a trans-activating CRISPR RNA (tracrRNA) and a Cas effector protein, pairing with both the target DNA and tracrRNA ¹⁴. One of the key features of CRISPR—Cas systems is the formation of a crRNA—Cas protein complex, which actively scans for complementary DNA sequences and degrades matching foreign nucleic acids^{25–27}. This defense mechanism begins with the RNase III-mediated processing of crRNA and tracrRNA into a functional RNA duplex. This duplex then associates with the Cas9 protein, facilitating R-loop formation and initiating endonuclease activity. Cas9, guided by this RNA complex, introduces a double-stranded break (DSB) at DNA sequences complementary to a 20-nucleotide spacer adjacent to a protospacer-adjacent motif (PAM)^{16,28}, a short conserved sequence of 2 to 5 base

pairs located close to the crRNA-targeted sequence, ^{6,29–31} critical for DNA target recognition and cleavage.

The CRISPR system has been further simplified by engineering a single-guide RNA (sgRNA) that combines both crRNA and tracrRNA into a single RNA molecule. This chimeric guide maintains full functionality and streamlines the use of Cas9 for targeted genome editing 16. By simply altering the spacer region of the sgRNA, the CRISPR-Cas9 system can be programmed to recognize virtually any DNA sequence, allowing for precise targeting and generation of site-specific bluntended double-strand break (DSB)¹⁶. The CRISPR-Cas9 protein derived from Streptococcus pyogenes (SpCas9) contains two critical nuclease domains, HNH and RuvC, which cleave the complementary and non-complementary strands of the target DNA^{32–34}. The mechanism of Cas9 activity can be divided into three key stages: target recognition, DNA cleavage, and repair. Initially, the guide RNA binds to the target DNA sequence and directs Cas9 to the specific genomic site. The Cas9-sgRNA complex scans for the presence of a PAM sequence, and upon recognition, Cas9 introduces a DSB at the target location. Once the DSB is formed, the cell attempts to repair the damage via one of two primary mechanisms: non-homologous end joining (NHEJ)³⁵, or homology directed repair (HDR)³⁶. NHEJ is a rapid but error-prone repair pathway that often results in small insertions or deletions (indels) at the cleavage site, leading to disruption of gene function, while HDR, on the other hand, is a more accurate repair process that uses a homologous DNA template to precisely restore the sequence 16,20,37–39.

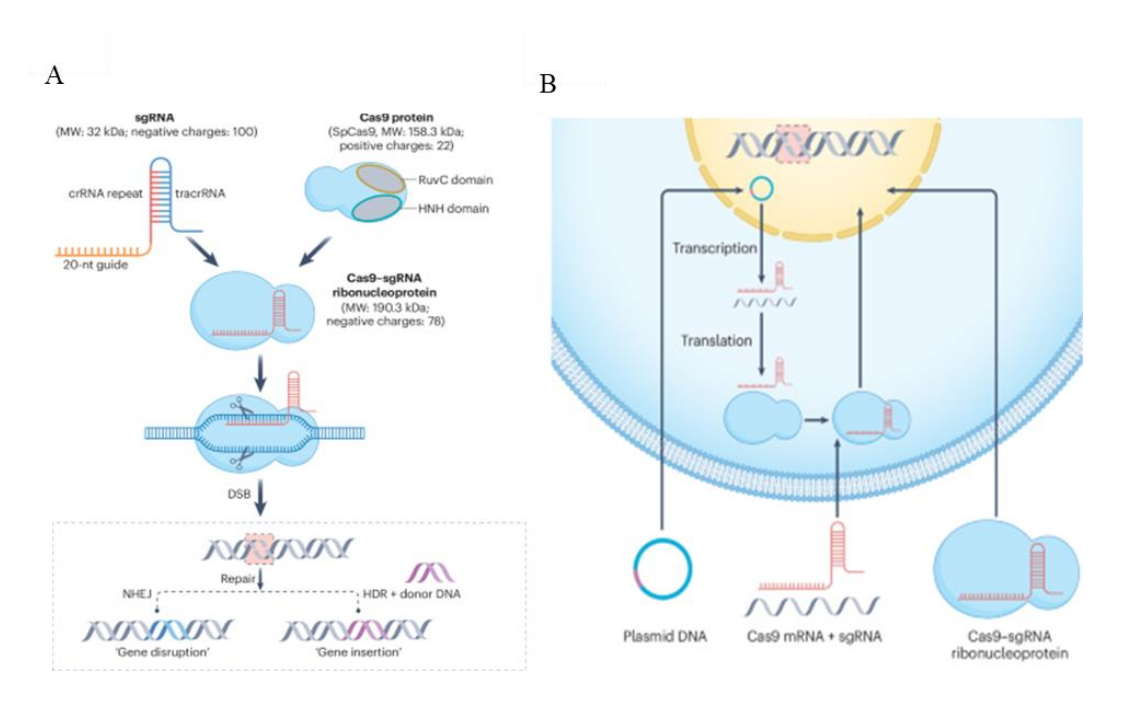


Figure 1 Mechanism and cellular delivery of CRISPR-Cas9 gene editing system.

(A) The CRISPR is consisted of Cas9 protein and single-guide RNA (sgRNA). The sgRNA guided Cas9 acts as molecular scissors to introduce a double-strand break (DSB) in the targeted DNA sequence using its RuvC and HNH nuclease domains. Together, the sgRNA and Cas9 form a ribonucleoprotein complex (RNP). The DSB can then be repaired by either nonhomologous end joining (NHEJ) or homology-directed repair (HDR). ((B) CRISPR components can be delivered in three main formats: plasmid DNA, Cas9 mRNA with sgRNA, and Cas9–sgRNA RNP complex. With plasmid DNA delivery, Cas9 is transcribed into Cas9 mRNA in the nucleus, transported with sgRNA to the cytoplasm for translation into Cas9 protein, and then The resulting Cas9–sgRNA RNP returns to the nucleus for editing. When delivering Cas9 mRNA with sgRNA directly, only translation is required before editing begins. In contrast, delivery of the Cas9–sgRNA RNP complex enables immediate gene editing upon entry into the cell, bypassing both transcription and translation steps. (Adapted from Alsaiari S.K. et al.⁴⁰)

2. CRISPR-Cas9 System Delivery Methods

While the CRISPR-Cas9 system has become a highly effective tool for genome editing, delivering its components into target cells remains a major obstacle. CRISPR/Cas9 can be delivered in three main forms: plasmid DNA (pDNA), messenger RNA (mRNA), or as a preassembled ribonucleoprotein (RNP) complex, each with distinct pros and cons⁴¹. Delivering pDNA or mRNA requires the host cell to perform transcription and/or translation before the CRISPR components become active, leading to a delayed onset of editing. Moreover, pDNA delivery often leads to persistent expression, which increases the risk of off-target effects and unintended genomic integration at double-strand break (DSB) sites^{41,42}. In contrast, Cas9 RNPs become active immediately after entering the cell and have a shorter half-life, minimizing the risk of off-target edits while enabling more precise and rapid genome editing^{43,44}. Because of these advantages, numerous delivery platforms have been developed to transport Cas9 RNPs, with EVs standing out as a high-potential option for translational use.

3. Carriers for Delivering CRISPR Technology

In vitro, plasmids or mRNA encoding CRISPR/Cas gene-editing components can be introduced into cells using conventional methods such as transfection reagents, viral vectors, or other standard delivery techniques. Similarly, RNPs are typically delivered into cells via electroporation. However, these approaches are often not well-suited for in vivo applications. For CRISPR tools to be effective in vivo, they must successfully navigate a complex, multi-step delivery process. First, the delivery vehicle must remain stable in the bloodstream, avoiding enzymatic degradation and immune system clearance. Second, it must selectively accumulate in the target tissue and promote cellular uptake through endocytosis. Finally, the CRISPR components must escape the endolysosomal pathway into the cytoplasm, where they can access the genome to induce edits or

regulate gene expression. Among these steps, targeted accumulation in the desired tissue is especially critical for achieving efficient and specific gene editing.

Viral delivery methods. Adeno-associated virus (AAV) is among the most widely used viral vectors for gene delivery due to its ability to efficiently cross species barriers and its low immunogenicity, which reduces the likelihood of provoking an inflammatory response⁴⁵. However, one of the major limitations of using AAV for delivering CRISPR/Cas9 is its limited packaging capacity, only about 4.7 kb, which is insufficient for the relatively large CRISPR/Cas9 components⁴⁶. While co-transfection strategies can be used to express Cas9 and sgRNA within the cell to regulate gene expression, this approach carries a higher risk of off-target effects. Lentiviral vectors, derived from retroviruses, are also commonly used for CRISPR delivery because they can infect both dividing and non-dividing cells⁴⁷. With a larger packaging capacity of approximately 10 kb, lentiviruses are capable of carrying the entire CRISPR/Cas9 system, but their tendency to integrate randomly into the host genome raises safety concerns, including the potential for immune responses and oncogenesis⁴⁸. Baculoviruses have also been explored as delivery vectors for CRISPR/Cas9. These are insect-specific viruses with a much larger cargo capacity (~38 kb)^{49,50}. Non-viral delivery methods. As alternatives to viral vectors for CRISPR-Cas9 delivery, non-viral delivery methods, including nanoparticles, electroporation, and microinjection, are being actively investigated.

Lipid nanoparticles (LNPs) consist of a lipid bilayer structure that mimics cell membranes and encapsulates an aqueous core. These systems can be engineered to improve target specificity and minimize off-target effects. However, their effectiveness is highly dependent on the cell type and may be hindered by limited stability and low transfection efficiency.

Polymer-based nanoparticles are another promising nonviral approach. They are typically made from biodegradable materials such as poly(lactic-co-glycolic acid) (PLGA), polyethyleneimine (PEI), PEG, or chitosan. These nanoparticles offer a range of advantages like low immunogenicity, good biocompatibility, and excellent encapsulation efficiency for nucleic acids. Their structure is highly customizable, allowing researchers to fine-tune size, surface charge, and drug release profiles to optimize delivery⁵¹. Particle size plays a crucial role in tissue penetration and cellular uptake, with smaller particles generally showing better performance. Surface charge can be adjusted to promote membrane interaction, while surface modifications can improve targeting specificity, further enhancing CRISPR-Cas9 delivery.

Electroporation delivers CRISPR components into cells by applying electrical pulses that create temporary pores in the cell membrane. While it offers high efficiency and enables delivery of large components like Cas9 protein and long guide RNAs, it can be harsh on cells and is less suitable for fragile or sensitive cell types⁵². Despite its drawbacks, electroporation remains a versatile tool with strong potential for applications requiring the delivery of complex gene-editing constructs. Exosomes, naturally occurring membrane-bound vesicles (30–100 nm in size), originate from multivesicular bodies and have emerged as a promising CRISPR delivery platform^{53,54}. These vesicles can directly package Cas9 and sgRNA, reducing the risk of off-target effects during transport. As endogenous carriers, exosomes are biocompatible and less likely to be cleared by the immune system compared to viral vectors, lipid-based systems, or synthetic nanoparticles. However, to effectively target specific cell types, particularly those that secrete few exosomes, exogenous modifications are often required. Technologies like genome editing with designed extracellular vesicles (GEDEX) have been developed to improve the delivery efficiency and precision of dCas9-based constructs such as dCas9/VPR⁵⁵.

Gold nanoparticles (AuNPs) also hold promise for CRISPR delivery due to their customizable size, excellent stability, and high biocompatibility. Their surfaces are easily modifiable, making them suitable carriers for gene-editing therapeutics⁵⁶.

Biomimetic nanomaterials are gaining interest due to their potential to enhance CRISPR-based therapies by remaining stable in circulation and accumulating at targeted tissue sites⁵⁷. However, synthetic carriers, whether organic or inorganic, are often partially cleared by the immune system *in vivo*. To address this, researchers are now exploring materials derived directly from the body.

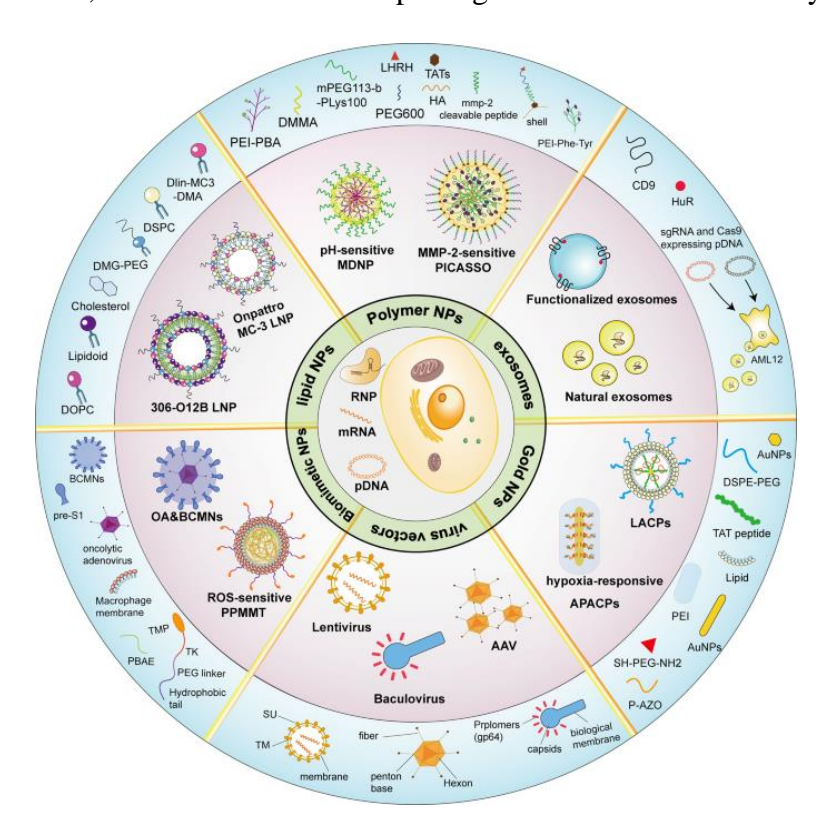


Figure 2 Overview of various delivery vectors used for *in vivo* CRISPR system administration.

The diagram illustrates three primary formats of CRISPR delivery at the center, including plasmid DNA (pDNA), messenger RNA (mRNA), and ribonucleoproteins (RNPs). Surrounding this center are examples of commonly used delivery carriers. The outermost ring highlights the origin,

production methods, or structural components of these carriers. SU denotes surface envelope protein, and TM refers to transmembrane envelope protein. (Adapted from Li et al.⁵⁸)

4. Limitations of Targeted Delivery

Off-target effects. Although CRISPR-Cas9 is engineered to edit specific genes, it can occasionally alter unintended genomic regions, raising serious concerns for its use in *in vivo* therapeutic applications^{59,60}. These unintended edits, known as off-target effects, are influenced by several factors, including the length and design of the guide RNA, the sequence of the target DNA, and the efficiency of the Cas9 enzyme. Research has shown that even highly specific guide RNAs can sometimes lead to off-target activity, and different variants of the Cas9 enzyme display distinct off-target profiles⁶¹.

Delivery efficiency and targeting. An ideal delivery system for CRISPR/Cas9 should be efficient, cause minimal immune responses, and successfully direct the Cas9/sgRNA complex to specific target cells or tissues. However, existing methods, such as viral vectors, electroporation, and lipofection, each present certain limitations, including inefficiency or cellular toxicity. Plasmid-based delivery systems also face challenges, particularly limited targeting capabilities and suboptimal control over Cas9 activity. In the case of adeno-associated viruses (AAVs), the primary drawback is their restricted cargo capacity⁶². Lentiviral vectors, while capable of delivering larger genetic material, are associated with safety risks and immunogenicity, which limit their suitability for therapeutic applications^{63,64}. Nanoparticle-based systems offer a non-viral alternative but often suffer from low gene-editing efficiency⁶⁵. Among non-viral techniques, methods such as microinjection, transfection, and electroporation show promise as delivery platforms for gene editing.

Large DNA fragment insertion and deletion. One of the key challenges of CRISPR-Cas9 technology is its limited ability to efficiently insert or delete large DNA fragments, typically beyond 1–2 kilobases. While the system performs well for small genetic edits, such as point mutations or short insertions and deletions, its effectiveness decreases significantly with larger modifications. This is primarily because it becomes more difficult for the Cas9 enzyme to accurately locate and cleave the intended site within the genome²⁰. Additionally, when working with larger DNA sequences, there is an increased risk of off-target activity, where Cas9 may inadvertently modify unintended regions of the genome, potentially leading to undesired genetic changes.

Mosaicism and heterogeneity. When applying CRISPR-Cas9 for gene editing, it's common for different cells within the same tissue or organism to exhibit varying levels of genetic modification, a phenomenon known as mosaicism. Mosaicism occurs when an organism contains more than one genetically distinct cell population. While it can occur naturally, it can also be unintentionally induced by gene-editing techniques like CRISPR-Cas9⁶⁶. This variability can lead to unintended genetic mutations, potentially undermining the precision of CRISPR edits and causing unpredictable outcomes, including the risk of disease development. Mosaicism complicates the ability to achieve uniform and consistent gene editing across all target cells, often resulting from differences in the timing, efficiency, or delivery of the CRISPR-Cas9 components.

In contrast, heterogeneity refers to broader genetic variation within an organism's genome. This genomic diversity can also impact the reliability of CRISPR-Cas9 by introducing unintended mutations, especially when genetic variability is influenced by factors such as age, environment, or underlying genetic conditions. Research indicates that such heterogeneity can compromise the

accuracy of CRISPR-based editing, making results less predictable and increasing the likelihood of off-target effects or unwanted genetic alterations⁶⁷.

Immune response and immunogenicity. One of the key concerns with CRISPR-Cas9 is its potential to trigger an immune response, which can reduce the effectiveness of gene editing and pose risks if the system is reintroduced into the bloodstream. To address this challenge, researchers have proposed several strategies to minimize CRISPR-Cas9's immunogenicity and the associated immune limitations. One of the methods involves modifying the Cas9 protein itself to make it less recognizable to the immune system, thereby reducing immunogenicity while maintaining or enhancing its editing efficiency.

5. Extracellular Vesicles (EVs) to Deliver CRISPR/Cas9

Extracellular vesicles (EVs) are nano-sized, lipid bilayer-enclosed particles that are naturally released by nearly all types of cells. They play a vital role in intercellular communication, helping maintain essential physiological processes by transporting a wide range of biological molecules⁶⁸. The lipid bilayer structure protects their cargo from damaging external factors, such as digestive enzymes, preserving the integrity of their contents during transport⁶⁹. Due to their unique properties, EVs are being actively explored both as diagnostic biomarkers and as potential therapeutic tools for a variety of diseases.

Biogenesis of EVs. EVs are generally categorized into three main types based on their origin and biogenesis: exosomes, ectosomes, and apoptotic bodies⁷⁰. Exosomes are small vesicles, typically ranging from 30 to 150 nanometers in diameter, and are formed within multivesicular bodies (MVBs). These are released when MVBs fuse with the plasma membrane⁷¹. In contrast, ectosomes also known as microvesicles are larger, usually between 100 and 1,000 nanometers, and are generated by direct outward budding and shedding from the cell's plasma membrane^{68,72,73}. The

tetraspanin family of proteins plays a key role in the formation of these vesicles, although their involvement varies between exosome and ectosome production⁷⁴. Apoptotic bodies, the third category, are produced during the process of programmed cell death (apoptosis), and consist of membrane-bound fragments released as cells break down⁷⁵.

Exosomes. Exosomes are formed through the inward budding of the endosomal membrane, a process that generates MVBs⁷⁶. These MVBs follow one of two fates: they can either fuse with lysosomes for degradation or merge with the plasma membrane to release their intraluminal vesicles, called exosomes, into the extracellular environment⁷². The formation of exosomes is orchestrated through multiple pathways, which are generally grouped into two main mechanisms: ESCRT-dependent and ESCRT-independent. In the ESCRT-dependent pathway, the formation of intraluminal vesicles (ILVs) is driven by a series of protein complexes—ESCRT-0, -I, -II, and -III along with associated proteins such as ALIX, TSG101, and VPS4⁷⁷. In contrast, the ESCRTindependent route involves the contribution of tetraspanin-enriched microdomains (TEMs) and lipid raft structures. Tetraspanins such as CD9, CD81, and CD63 are key components of these domains and play essential roles in selecting and sorting cargo for exosome packaging⁷⁸. Recent research has also highlighted the involvement of the endoplasmic reticulum (ER) in exosome biogenesis. At membrane contact sites between the ER and late endosomes, the ER helps regulate endosome movement and maturation, a process closely linked to the action of small GTPases. These interactions are essential for the eventual fusion of MVBs with the plasma membrane and the release of exosomes⁷⁹. Small Rab GTPases, including RAB27a/b, RAB11, RAB7, and RAB35, are pivotal in regulating vesicle budding, trafficking, and movement, thus enabling MVBs to reach and fuse with the plasma membrane. Additionally, proteins such as SNAREs (e.g., VAMP7, YKT6) are crucial for the membrane fusion process⁸⁰. Other important contributors include

syndecan heparin sulfate proteoglycans, phospholipase D2 (PLD2), ADP ribosylation factor 6 (ARF6), and syntenin, all of which play regulatory roles in exosome biogenesis and release⁸¹.

Ectosomes. Ectosomes, a distinct class of extracellular vesicles, are generated through the outward budding of the plasma membrane. Their formation involves complex remodeling of both the membrane structure and cytoskeletal components^{82,83}. During the initial budding phase, proteins carrying lipid anchor modifications, such as myristoylation and palmitoylation, accumulate within the budding site, promoting membrane curvature necessary for vesicle formation⁸⁴. In parallel, transmembrane proteins and specific lipids aggregate within defined membrane microdomains, while subunits of the ESCRT-I complex are actively recruited to these budding sites on the plasma membrane⁸⁵. The small GTPase ARF plays a regulatory role in organizing cargo selection and driving ectosome secretion⁸⁶. As the budding process advances, ectosomes must be severed from the plasma membrane. This final step involves cytoskeletal loosening, which aligns with the incorporation of cytosolic proteins and RNAs into the forming vesicles⁸⁴. Intracellular calcium (Ca²⁺) levels are known to trigger membrane reorganization and cytoskeletal disassembly, while ESCRT-III complexes are essential for the membrane scission required to release mature ectosomes^{87,88}.

Other types: apoptotic bodies, exomers, etc. In addition to exosomes and ectosomes, other types of extracellular particles include apoptotic bodies and nonvesicular nanoparticles such as exomeres. Apoptotic bodies are released by cells undergoing the final stages of programmed cell death (apoptosis) and were once considered to be simply cellular debris⁸⁹. These vesicles vary widely in size, typically ranging from 50 nanometers to 3 micrometers, and may carry fragmented DNA, histones, or immature glycoepitopes. When taken up by recipient cells, apoptotic bodies can elicit anti-inflammatory or immunotolerant responses⁹⁰. Although the detailed mechanisms and

genetic regulators behind apoptotic body formation remain unclear, recent studies suggest that they arise through a controlled process known as apoptotic cell disassembly, which involves a sequence of well-orchestrated morphological changes⁹¹. More recently, researchers have identified exomeres and supermeres as novel nonvesicular nanoparticles, generally smaller than 50 nanometers in diameter. Exomeres are distinguished by their unique protein composition and tissue distribution, setting them apart from small extracellular vesicles. Similarly, supermeres are rich in RNA content and demonstrate greater accumulation in tissues compared to both exomeres and small EVs⁹².

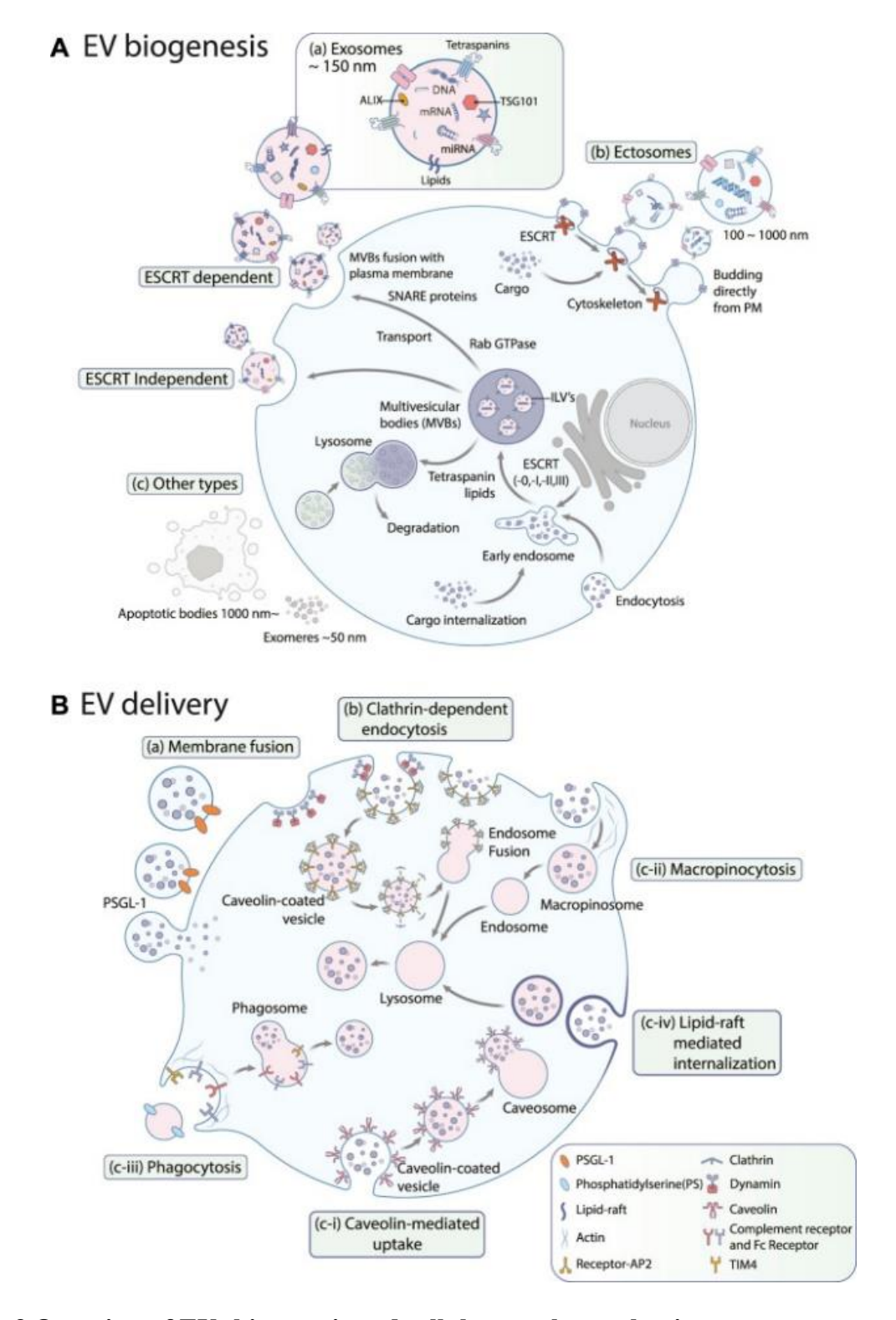


Figure 3 Overview of EVs biogenesis and cellular uptake mechanisms.

(A) EVs are primarily classified into three categories: (a) exosomes, (b) ectosomes, and (c) other vesicle types such as apoptotic bodies and exomeres. Exosome formation involves two main

pathways: (a-i) an ESCRT-dependent route and (a-ii) an ESCRT-independent mechanism. PM: plasma membrane. (B) Cellular internalization of exosomes can occur through several uptake pathways: (a) direct membrane fusion, (b) clathrin-mediated endocytosis, and (c) clathrin-independent mechanisms, which include (c-i) caveolin-mediated uptake, (c-ii) macropinocytosis, (c-iii) phagocytosis, and (c-iv) lipid raft-dependent internalization. Abbreviations: PSGL-1 = P-selectin glycoprotein ligand-1; PS = phosphatidylserine; AP2 = adipocyte protein 2; TIM4 = T-cell immunoglobulin and mucin domain-containing protein 4. (Adapted from Yu et al. ⁹³).

6. Extracellular Vesicles Delivery

The method by which EVs are taken up is influenced by both the type of EVs and the characteristics of the recipient cell. Generally, EVs uptake occurs through one of three main routes: membrane fusion, clathrin-mediated endocytosis, and clathrin-independent endocytosis, which includes pinocytosis and phagocytosis. Additionally, lipid rafts and specific protein–protein interactions have been found to facilitate and regulate the internalization process⁹⁴.

Cell membrane fusion. One of the simplest and most direct ways that extracellular vesicles (EVs) are internalized is through membrane fusion, where the EVs membrane merges directly with the plasma membrane of the recipient cell. This pathway allows for the immediate delivery of both internal and membrane-bound cargo into the target cell without passing through endocytic or lysosomal routes⁹⁵.

Clathrin-dependent endocytosis. This process begins at the plasma membrane, where clathrin-coated pits are formed. EVs are then internalized within clathrin-coated vesicles through a scission event mediated by the large GTPase dynamin, which separates the neck of the budding vesicle⁹⁶. Once inside the cell, the clathrin coat is shed, allowing the EVs-containing vesicles to merge with endosomes and continue through the endocytic pathway ⁹⁷.

Caveolin-mediated uptake. Caveolin-mediated uptake operates through the formation of small invaginations in the plasma membrane known as caveolae. These structures are formed through the expression of caveolin, a small integral membrane protein. Each caveola contains caveolin-1 molecules that function by forming dimers and recruiting cavin proteins (CAVIN1, CAVIN2, CAVIN3, and CAVIN4) to stabilize and support the caveolar structure. Additionally, caveolin-1 has a strong affinity for cholesterol, facilitating its transport to the cell surface and its role in intracellular trafficking. Caveolar vesicles are notably well-organized and are rich in specific membrane lipids, including saturated phospholipids, sphingolipids, plasmenylethanolamines, and cholesterol⁹⁸.

Macropinocytosis. Macropinocytosis is a form of endocytosis characterized by the creation of large, actin-driven membrane ruffles known as macropinosomes. These protrusions extend outward from the cell membrane to engulf surrounding extracellular fluid and materials, forming large vesicles that are brought into the cell. Once inside, macropinosomes fuse with endosomes, enabling the internalized contents to be processed and used by the cell. This pathway is particularly active in certain cell types, such as macrophages and microglia, which are essential for immune defense and the removal of cellular debris.

Phagocytosis. Phagocytosis is a receptor-mediated cellular process that enables the uptake of large particles without the need for direct interaction with the cargo or the formation of membrane ruffles and is also used for the internalization of EVs⁹⁹. Phagocytic cells are particularly efficient at internalizing EVs via this mechanism¹⁰⁰, and their efficiency largely depends on the differentiation state of the phagocytes¹⁰¹. One of the key factors aiding in EVs uptake through phagocytosis is phosphatidylserine (PS), a phospholipid that is enriched on the outer surface of EVs membranes and thought to play a significant role in facilitating entry into recipient cells¹⁰². Additionally,

phosphoinositide 3-kinases (PI3Ks) are crucial for enabling membrane insertion during phagosome formation.

Lipid raft-mediated internalization. Lipid rafts are specialized, detergent-resistant microdomains within the plasma membrane ⁹⁴ that are rich in cholesterol, glycosphingolipids, and glycosylphosphatidylinositol (GPI)-anchored proteins. These domains serve as key platforms for organizing signaling molecules ¹⁰³ and have been implicated in the uptake of EVs.

7. CRISPR/Cas9 Delivery via EVs

EVs have emerged as a highly promising alternative for delivering CRISPR/Cas9 components, effectively overcoming many of the limitations posed by traditional delivery systems. Their natural biocompatibility and structural stability stem from their phospholipid bilayer membranes, which help protect cargo molecules, and from the presence of abundant surface signaling molecules. This protective structure helps the cargo avoid rapid degradation and clearance, allowing for prolonged circulation time in the body^{104–106}. Due to their modifiability, low immunogenicity, and efficient uptake, EVs are considered a safe and practical option for delivering a wide array of therapeutic molecules^{4,5}. Targeted delivery can be achieved by exploiting naturally occurring surface ligands or membrane proteins present on EVs¹⁰⁷. Additionally, stimuli-responsive cargo release offers precise spatial and temporal control, making EVs suitable for fine-tuned therapeutic applications ¹⁰⁸. Furthermore, cell adhesion molecules on the EVs surface facilitate their movement across biological barriers and into tissue regions with limited blood supply, which enhances both targeting accuracy and bioavailability 109,110. Thus, EVs show great potential as natural carriers for the delivery of CRISPR/Cas9 components. However, efficient transport to specific target sites remains a challenge, as both internal and external biological barriers can limit their effectiveness. Despite their in vivo advantages over viral vectors like AAVs and synthetic systems like lipid nanoparticles (LNPs), EVs-based delivery of CRISPR systems remains in the preclinical stage. Nevertheless, the clinical success of AAVs and LNPs for CRISPR delivery has encouraged the exploration of EVs for therapeutic applications in human diseases.

In terms of loading cargo into or onto EVs, there are generally three strategies, (1) Pre-loading (cell-based or pre-isolation method): This involves introducing cargo into parent cells, which then package and release it within EVs. Techniques like transfection¹¹¹ or co-incubation¹¹² are used. Although relatively simple and reproducible, this method often suffers from low loading efficiency, and outcomes vary depending on the parent cell type, cargo properties, and concentration gradients. (2) Post-loading (direct or post-isolation method): In this approach, EVs are first isolated and then loaded with cargo through techniques such as co-incubation⁴, electroporation¹¹³, sonication, extrusion¹¹⁴, transfection reagents¹¹⁵, or freeze—thaw cycles¹¹⁶. This method offers greater control over the loading process and reduces contamination from unwanted cellular components. (3) Other innovative techniques include the use of cellular nanoporation biochips¹⁰⁵, enveloped protein nanocages (EPNs), and synthetic or artificial EVs, which are being actively explored to improve precision and efficiency.

This study aims to evaluate the potential of extracellular vesicles (EVs) as a safe and effective delivery system for CRISPR/Cas9 ribonucleoprotein complexes to achieve *in vitro* and *in vivo* gene editing. Using EVs, especially those coated with viral envelope proteins like VSV-G, but not spike protein, may overcome current delivery barriers, offering a biocompatible, non-viral alternative vehicle for precise genome editing applications.

CHAPTER 2

EXPERIMENTAL METHODS

1. Cell Culture

The HEK293T (293T) cell line was obtained from the American Type Culture Collection (ATCC) and cultured in Dulbecco's Modified Eagle's Medium (DMEM; Cytiva, Cat No: SH30243.01). The growth medium was supplemented with 5% fetal bovine serum (FBS; Omega Scientific, Cat No: FB-01), 1% penicillin-streptomycin (Cytiva, Cat No: SV30010), and 1% GlutaMAXTM-1 (100X; Thermo Fisher, Ref: 35050-61) to maintain optimal cell growth conditions. All cell cultures were incubated at 37°C in a humidified atmosphere containing 5% CO₂, and cells were used for experiments up to 20 passages.

To generate 293T-eGFP cells that stably express enhanced green fluorescent protein (eGFP), parental 293T cells were transduced with the eGFP gene using a FUCGW lentiviral vector, generously provided by Dr. Owen Witte's laboratory. These transduced cells were cultured under the same conditions in DMEM supplemented with 5% FBS, 1% penicillin-streptomycin, and 1% GlutaMAXTM-1, and maintained at 37°C with 5% CO₂.

2. Plasmids Preparation

Lentiviral and non-lentiviral plasmid constructs encoding N-myristoylated, modified Cas9 (mCas9) were previously generated¹¹⁷. The SARS-CoV-2 spike protein sequence containing the D614G mutation and a 21-residue deletion at the C-terminus [designated as spike(D614G-Δ21)] was obtained from Addgene (plasmid #158762)^{118,119}. The plasmids including pMDL (8,895 bp) and VSV-G (7,631 bp) were generously provided by Dr. Owen Witte's laboratory. For plasmid

amplification, all constructs were transformed into One ShotTM TOP10 chemically competent E. coli (Invitrogen, Cat No: C4040-10). Transformed bacteria were plated onto LB agar plates containing 100 μg/mL carbenicillin and incubated overnight at 37°C. Single colonies were then selected and grown in 250 mL LB broth with 100 μg/mL carbenicillin under shaking conditions (250 rpm at 37°C overnight). Plasmid DNA was isolated and purified using the E.Z.N.A.® Plasmid DNA Maxi Kit (OMEGA BIO-TEK, Cat No: D6922-04). The DNA concentration and purity were measured using a NanoDropTM Lite Spectrophotometer (Thermo ScientificTM, ND-LITE-PR), with A260/A280 ratios between 1.80 and 1.90, indicating high purity. All plasmid preparations were stored at -20°C until further use.

3. Protein Extraction and Western Blotting

Protein lysates were prepared from cultured cells using RIPA buffer (composition: 50 mM Tris-HCl, pH 7.4; 150 mM NaCl; 1% NP-40; 0.5% sodium deoxycholate; 0.1% SDS; Biosciences®, Cat#: 786-489), supplemented with a protease inhibitor cocktail in a 100:1 ratio (RIPA:PI). Cells were incubated on ice for 20 minutes to lyse, then vortexed for 5 minutes to ensure complete disruption. Lysates were centrifuged at 21,000 × g for 15 minutes, and the supernatants were collected. Protein concentrations were measured using 5 μL of each lysate via the detergent-compatible (DC) colorimetric protein assay (Bio-Rad, Cat#: 500-0114), following the manufacturer's guidelines. Remaining lysates were mixed with 6X Laemmli buffer and denatured by heating at 95°C for 5 minutes. For EVs protein analysis, the samples were directly lysed in 6X Laemmli buffer and similarly boiled. Equal protein amounts from cell lysate (20 μg per lane) and equal number of EVs particles were resolved by SDS-PAGE using a 10% resolving gel with a 4% stacking gel. Electrophoresis was run at 80 V for 30 minutes, followed by 120 V for 80 minutes in Tris-glycine-SDS running buffer. Proteins were transferred onto nitrocellulose (NC) membranes

via wet transfer (Bio-Rad system) using a transfer buffer (25 mM Tris, 192 mM glycine, 20% methanol) at 98 V for 90 minutes. Membranes were blocked in 5% non-fat dry milk in TBS for 1 hour at room temperature, then incubated overnight at 4°C with primary antibodies diluted in the same blocking buffer with gentle agitation. Primary antibodies were diluted as described below in 5% milk TBS. The following primary antibodies were used as recommended by the manufacturer: Rabbit anti-calnexin (Cat#: 2679, 1:1000), and mouse anti-Cas9 (Cat#: 14697, 1:1000) were purchased from Cell Signaling Technology. Mouse anti-VSV-G (Cat#: EB0010, Kerafast, 1:1000), rabbit anti-syntenin (Cat#: ab19903, Abcam, 1:1000), mouse anti-CD63 (Cat#: 556019, BD Pharmingen, 1:1000), and mouse-anti-c-SRC (Cat#: 60315-1-Ig, Proteintech, 1:5000. The next day, the membranes were washed 5 times over 25 minutes with TBST (TBS + 0.1% Tween 20). The secondary antibodies were diluted in 5% milk TBS as described below and the membranes were incubated for 1 h at room temperature with gentle agitation. Secondary antibodies anti-rabbit IgG HRP (Cat#: 7074, 1:2000) and anti-mouse IgG HRP (Cat# 7076, 1:2000) were purchased from Cell Signaling Technology. Following secondary antibody incubation, membranes were washed three times over 30 minutes with TBST. Protein bands were visualized using Cytiva Amersham ECL chemiluminescence reagents (Cat#: 45-000-878) and X-ray film exposure.

4. Polymerase Chain Reaction (PCR) and DNA Sequencing

Cells from both EVs-treated and untreated control groups were harvested by trypsinization, followed by centrifugation at 1100 RPM for 5 minutes at 25°C. The resulting cell pellets were washed with sterile 1X phosphate-buffered saline (PBS) to remove residual media. Genomic DNA (gDNA) was extracted using the GeneJET Genomic DNA Purification Kit (Thermo Fisher, Cat# K0721), following the manufacturer's instructions. The extracted gDNA was then used as a template for PCR amplification targeting the sgRNA-eGFP binding region. The following two

primers, eGFP forward primer 5' – GGTCTTGTAGTTGCCGTCGTCCTT – 3' and 5' – GATCGCCTGGAGACGCCATC – 3', and eGFP reverse primer 5' – AGCTCGTTTAGTGAACCGTCAGAT – 3' were used for PCR amplification. PCR reactions were performed using Q5® High-Fidelity DNA Polymerase (New England Biolabs, Cat# M0491S). Each 25 μL reaction contained 1 μg of genomic DNA and 2 U/μL of polymerase, prepared according to the manufacturer's protocol. Amplification was carried out using a Bio-Rad C1000 TouchTM Thermal Cycler under conditions specified by the enzyme manufacturer.

After amplification, PCR products were purified using the QIAquick® PCR Purification Kit (Qiagen, Cat# 28104). For Sanger sequencing, the purified PCR product was sequenced using the eGFP forward primer (5' – GGTCTTGTAGTTGCCGTCGTCCTT – 3' or 5' – GATCGCCTGGAGACGCCATC – 3'). For Next Generation Sequencing (NGS), amplified products were first separated on a 1% agarose gel, and the desired DNA band was excised and purified using the QIAquick® Gel Extraction Kit. Both Sanger and NGS analyses were performed by Azenta Life Sciences to evaluate the efficiency of eGFP gene editing.

5. T7 Endonuclease Assay

T7 endonuclease assay was performed using the GeneArtTM Genomic Cleavage Detection Kit (Thermo Fisher Scientific, Cat# A24372) following the manufacturer's protocol to evaluate genome editing efficiency. Purified PCR products surrounding the sgRNA-eGFP target site were first subjected to melting and reannealing process to allow heteroduplex formation. Following reannealing, the DNA was incubated with T7 endonuclease (10 U/μL) enzyme at 37°C for 60 minutes in a total reaction volume of 20 μL. Cleavage products were separated by electrophoresis on a 2% agarose gel containing a DNA stain (ethidium bromide) and visualized under UV illumination. The presence of cleavage bands indicated insertions or deletions (indels).

6. Production and Isolation of EVs Encapsulating mCas9/sgRNA-eGFP and Coated with VSV-G and/or Spike(D614G- Δ 21)

A total of 6.25 x 10⁶ HEK293T cells were seeded into a 15-cm culture dish, respectively and maintained in Dulbecco's Modified Eagle's Medium (DMEM) as recommended by ATCC, supplemented with 5% fetal bovine serum (FBS), 1% penicillin-streptomycin, and 1% GlutaMAXTM-1 (100X). The cultures were incubated at 37°C in a humidified 5% CO₂ atmosphere. The following day, the medium was refreshed with DMEM containing 5% FBS and 1% GlutaMAXTM-1, and cells were returned to the incubator. For EVs production, cells were cotransfected with 50 µg of mCas9/sgRNA-eGFP plasmid and 10 µg of pCMV-VSV-G or spike(D614G- Δ 21) plasmid using the calcium phosphate transfection method. Approximately 16 hours' post-transfection, the transfection media was replaced with fresh medium [supplemented with 5% fetal bovine serum (FBS), 1% penicillin-streptomycin, and 1% GlutaMAXTM-1 (100X)]. The conditioned medium was collected and sequentially centrifuged to eliminate cellular debris first at $2,000 \times g$ for 15 minutes, followed by $10,000 \times g$ for 35 minutes at 4°C. The resulting supernatant was passed through a 0.80-µm pore-size filter to further remove residual debris. For concentrated EVs, the filtered medium was ultracentrifuged at 100,000 × g for 2 hours at 4°C using a SW32Ti rotor (Beckman Coulter). After centrifugation, approximately 100 µL of the supernatant was carefully removed, and the EVs pellet was gently resuspended in the remaining medium following overnight storage at 4°C. The freshly isolated EVs were either used immediately for downstream applications, characterized, or stored at -80°C for up to two months for future use.

7. EVs Characterization and Size Distribution

To characterize the EVs, each isolated sample was diluted 1:1000 in sterile 1X phosphate-buffered saline (PBS, pH 7.4). The diluted samples were gently vortexed for 10–15 seconds to ensure

uniform mixing before analysis. The size distribution and particle concentration of the EVs were evaluated using the NanoSight Pro Nanoparticle Tracking Analysis (NTA) system (Malvern Panalytical, UK), operated with its dedicated software. The diluted EV suspension was loaded into the instrument's sample chamber using a sterile syringe. For each sample, five individual video recordings were captured, and the median particle size along with the particle concentration (particles/mL) was determined by averaging the results from all five videos.

8. EVs Mediated Genome Editing in HEK293T-eGFP Cells

The eGFP gene knockout efficiency of the EVs coated with VSV-G and encapsulating mCas9/sgRNA targeting eGFP was determined *in vitro*. HEK293T-eGFP cells were seeded at a density of 5 × 10⁴ cells per well in 12-well plates and cultured in 2 ml of DMEM media with 5% FBS. Cells were maintained at 37°C in a humidified incubator with 5% CO₂ overnight to allow for attachment prior to treatment with EVs. Next day, the media was replaced with 500 μl of fresh DMEM media containing polybrene (8 μg/ml), and 100 μl of EVs (containing 1 × 10¹¹ EVs particles) added to each well. After 24 hours of incubation at 37°C, 500 μL of additional fresh DMEM was added to each well, and the cells were incubated for another 24 hours. The confluent cells were then passaged, and re-seeded for a second round of EV treatment under identical conditions. HEK293T-eGFP cells were imaged by fluorescent microscopy after 7 days' post-treatment. Cells were harvested by trypsinization, centrifuged at 1100 rpm for 5 minutes at 25°C, washed with sterile 1X PBS (pH 7.4), and the cell pellets were stored at -80°C for further analysis.

9. In Vivo Endogenous eGFP Gene Editing in Various Organs of NOD-SCID-EGFP Mouse Using EV-Encapsulated CRISPR/Cas9 RNPs

To evaluate the eGFP gene knockout efficiency of the EVs coated with VSV-G and encapsulating mCas9/sgRNA targeting eGFP for *in vivo* gene editing, we utilized the NOD.Cg-*Prkdc*^{scid}

Il2rg^{tm1Wjl} Tg(CAG-EGFP)1Osb/SzJ (NSG-EGFP) mouse strain (Strain #:021937, Jackson Laboratory). These immunodeficient mice are characterized by the features of the NOD/ShiLtJ background, the severe combined immune deficiency mutation (SCID) and IL2 receptor gamma chain deficiency and a transgene harboring an enhanced green fluorescent protein (EGFP). The absence of functional T cells, B cells, and natural killer (NK) cells, as well as impaired cytokine signaling allows them for efficient engraftment of human cells.

This group aimed to evaluate the genome editing capacity of EVs in non-tumor tissues to target endogenous eGFP gene in various organs. The *in vivo* study consisted of four independent experiments. In each experiment, two NOD-SCID EGFP mice were used: one control (n=1) and one treatment (n=1). At least two months old mice were used for the experiments. The NSG-EGFP mice were intravenously administered EVs coated with VSV-G and encapsulating mCas9/sgRNA targeting the eGFP (treatment group) or EVs expressing only VSV-G (control group). Each mouse received 200 µL of EVs solution via tail vein injection. The dosing schedules were every other day injection over 11 days (total 6 doses) and 14 days (total 7 doses) for Experiment 1 and 2, respectively, and daily injection over 16 days (total 16 doses) and 24 days (total 24 doses) for Experiment 2 and Experiment 3, respectively.

After a 7-day observation period of post-treatment after the final dose, mice were euthanized, and major organs were harvested, including the liver, lung, heart, brain, kidney, pancreas, prostate, and small intestine. The organs were washed thoroughly with 1× PBS. Approximately one-third of each organ was snap-frozen and stored at -80°C for downstream genomic analysis. The remaining tissues were fixed in 10% buffered formalin phosphate (fisher chemical, Lot# 235853) for 72 hours, then transferred to 70% ethanol (DLI, Lot#2062411) and stored at room temperature. Genomic DNA from liver and lung tissues was extracted using GeneJET Genomic DNA

Purification Kit (thermos scientific, Lot# 3119304), quantified using NanoDrop[™] Lite Spectrophotometer (Thermo Scientific[™], ND-LITE-PR), with A260/A280 ratios between 1.80 and 1.90, indicating high purity, and submitted for both Sanger sequencing and Next Generation Sequencing (NGS) to determine INDEL formation at the eGFP locus.

10. In Vivo eGFP Gene Editing in Xenograft Tissues in NOD-SCID-EGFP Mouse Using EVs Encapsulated CRISPR/Cas9 RNPs

To explore eGFP gene editing efficiency of EVs Encapsulated CRISPR/Cas9 RNPs, same as described above NOD-SCID-EGFP mice were used. The study consisted of one experiment. The subcutaneous xenograft models were implanted by injecting eGFP expressing 293T or C4-2B cells into NOD-SCID-EGFP mice. Both control and treatment mice received subcutaneous injections of 1x10⁶ 293T and C4-2B eGFP cells. Once visible tumors formed, mice were treated with the EVs encapsulated mCas9/sgRNA plasmid targeting eGFP gene and enveloped with VSV-G (treatment) or EVs with only VSV-G (control). All injections were administered intravenously at a volume of 200 μL per dose. Treatment schedules were daily injection over 08 days. After treatment, the mice were euthanized. Xenograft tissues and major organs were harvested, washed with 1x PBS, and processed similarly as described above. A portion of each xenograft tissue and organ was frozen at −80°C, while the remainder was fixed in 10% buffered formalin phosphate (fisher chemical, Lot# 235853) for 72 hours, then transferred to 70% ethanol (DLI, Lot#2062411) and stored at room temperature. Genomic DNA was extracted from xenograft tissues and analyzed by Sanger sequencing and NGS to evaluate the gene editing efficiency.

11. Statistical Analysis

The data of particle size distribution was obtained from NanoSight Pro Nanoparticle Tracking Analysis (NTA) system (Malvern Panalytical, UK), operated with its dedicated software. Then

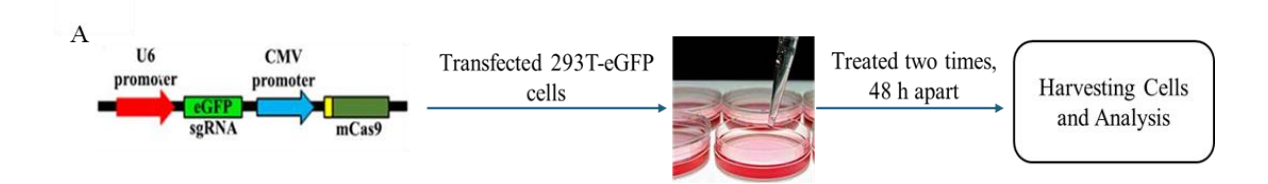
the data were subjected to statistical analysis by Prism 9.5.1. Paired t-test was carried out (*: p < 0.05; **: p < 0.01; ***: p < 0.001; ns: not significant).

CHAPTER 3

RESULTS

1. mCas9/sgRNA Plasmid Targeting the eGFP Gene Induced Efficient Gene Editing in HEK293T-eGFP Cells

To assess CRISPR/Cas9-mediated gene editing efficiency targeting the eGFP gene *in vitro*, HEK293T-eGFP cells were transfected with a plasmid expressing mCas9 and sgRNA-eGFP (Figure 4A). After transfection, eGFP fluorescence was evaluated in recipient cells using fluorescence microscopy. A noticeable loss of green fluorescence was observed in cells receiving the mCas9/sgRNA-eGFP plasmid, suggesting disruption of the eGFP gene expression (Figure 4B). In contrast, untransfected control cells showed no loss of eGFP expression (Figure 4B). To confirm the genome editing, genomic DNA was isolated from transfected cells and analyzed by Sanger sequencing. The sequencing results showed insertion-deletion (INDEL) mutations at the Cas9 target site with an overall editing efficiency of 34% (Figure 4C). No INDELs were identified in the control group (Figure 4C), confirming the specificity of the mCas9/sgRNA plasmid. These results demonstrate that transfection with the mCas9/sgRNA-eGFP plasmid leads to efficient gene editing in HEK293T-eGFP cells.



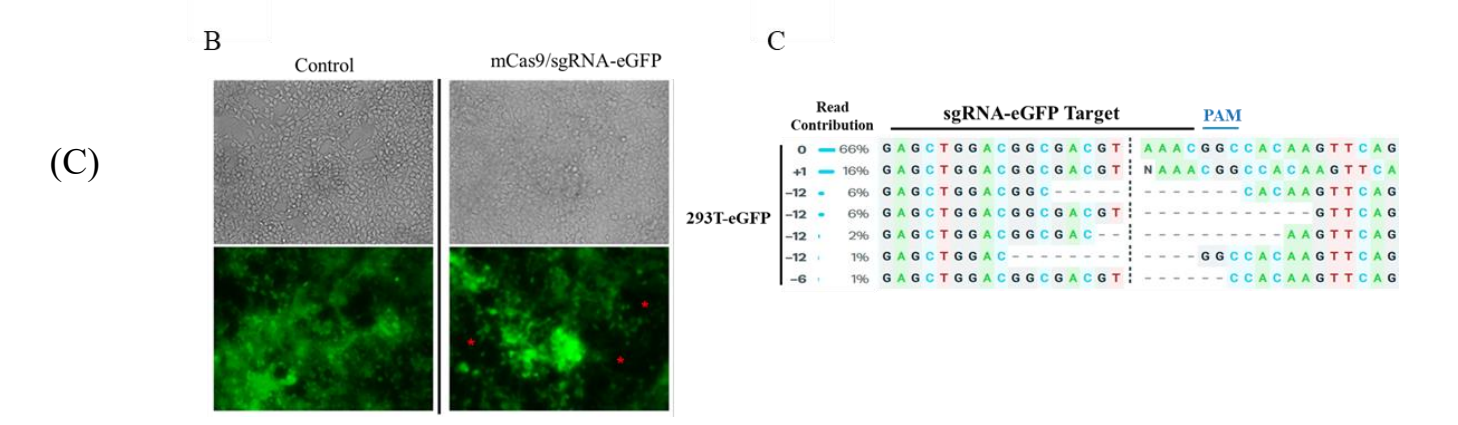


Figure 4 eGFP gene knockout in HEK293T-eGFP cells using mCas9/sgRNA plasmid.

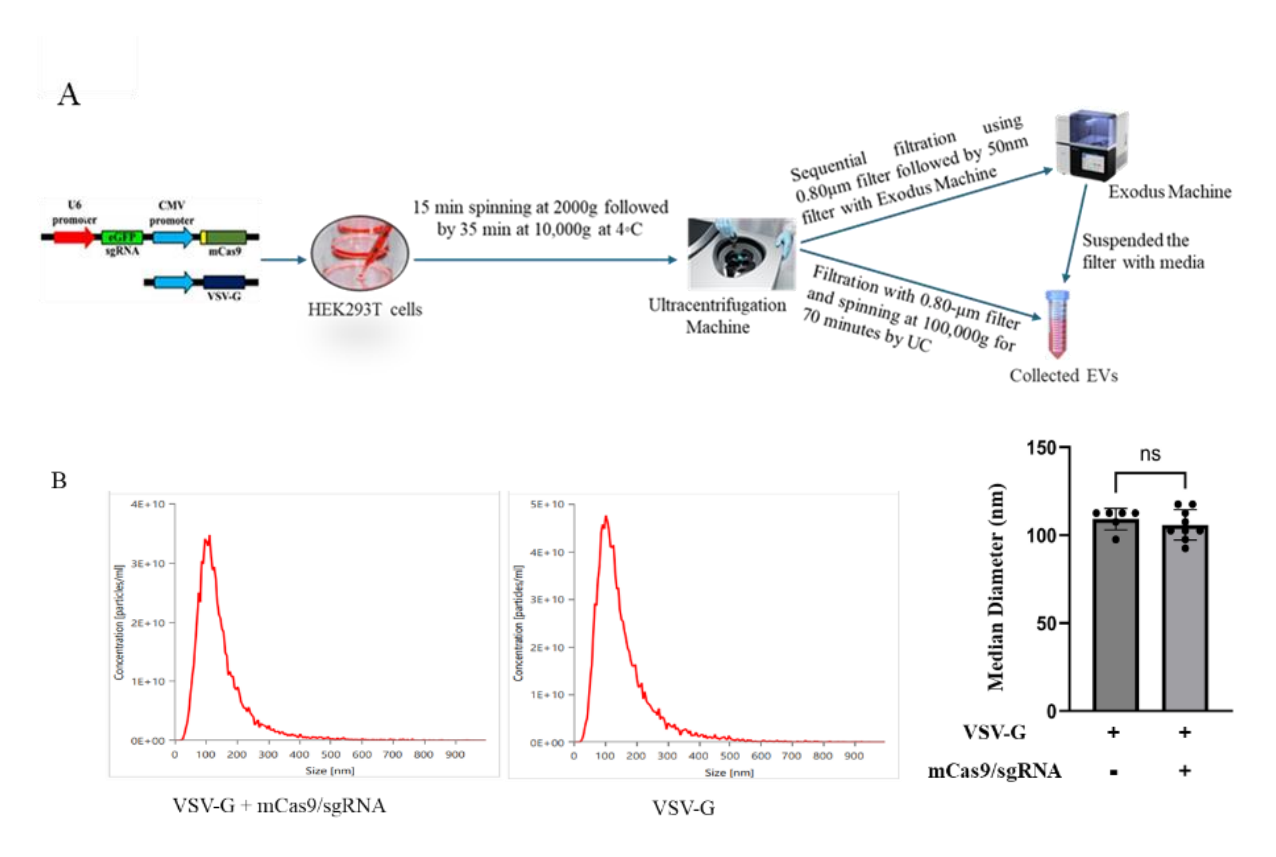
(A) HEK293T-eGFP cells were transfected twice, 48 hours apart, with a total of 17 μg of non-lentiviral plasmid encoding mCas9 and sgRNA targeting eGFP. (B) The transfected cells were subjected to fluorescent microscopy analysis at seven days' post-transfection. The cells with absent green fluorescence, indicative of gene knockout, are marked with red asterisks. (C) The extracted genomic DNA from transfected cells was amplified via PCR and analyzed by Sanger sequencing.

2. Isolation and characterization of EVs and confirmation of VSV-G and mCas9 expression in the EVs.

HEK293T cells were transfected with VSV-G alone and in combination with mCas9/sgRNA vectors (Figure 5A). The average of the median diameter of the isolated EVs were at 109.2±6.06 nm for the VSV-G group and 105.8±8.66 nm for the VSVG + mCas9/sgRNA group, which had no significantly difference (p≤0.05) Figure 5B).

As expected, Cas9, myristoylated Cas9, and VSV-G were detected only in the VSVG + mCas9/sgRNA groups (isolated by UC or Exodus), but not in 293T cell lysate (Figure 5C). Notably, UC-isolated EVs displayed higher expression levels of syntenin, Cas9, and myristoylated Cas9 compared to Exodus-isolated EVs. The detection of positive EVs protein biomarkers such as syntenin and CD63, and by the absence of the endoplasmic reticulum protein calnexin suggests

the purity of the EVs (Figure 5C). TEM of EVs isolated by both methods showed the expected cup-shaped morphology (Figure 5D). Overall, the data indicate that VSV-G and mCas9/sgRNA are co-incorporated into EVs.



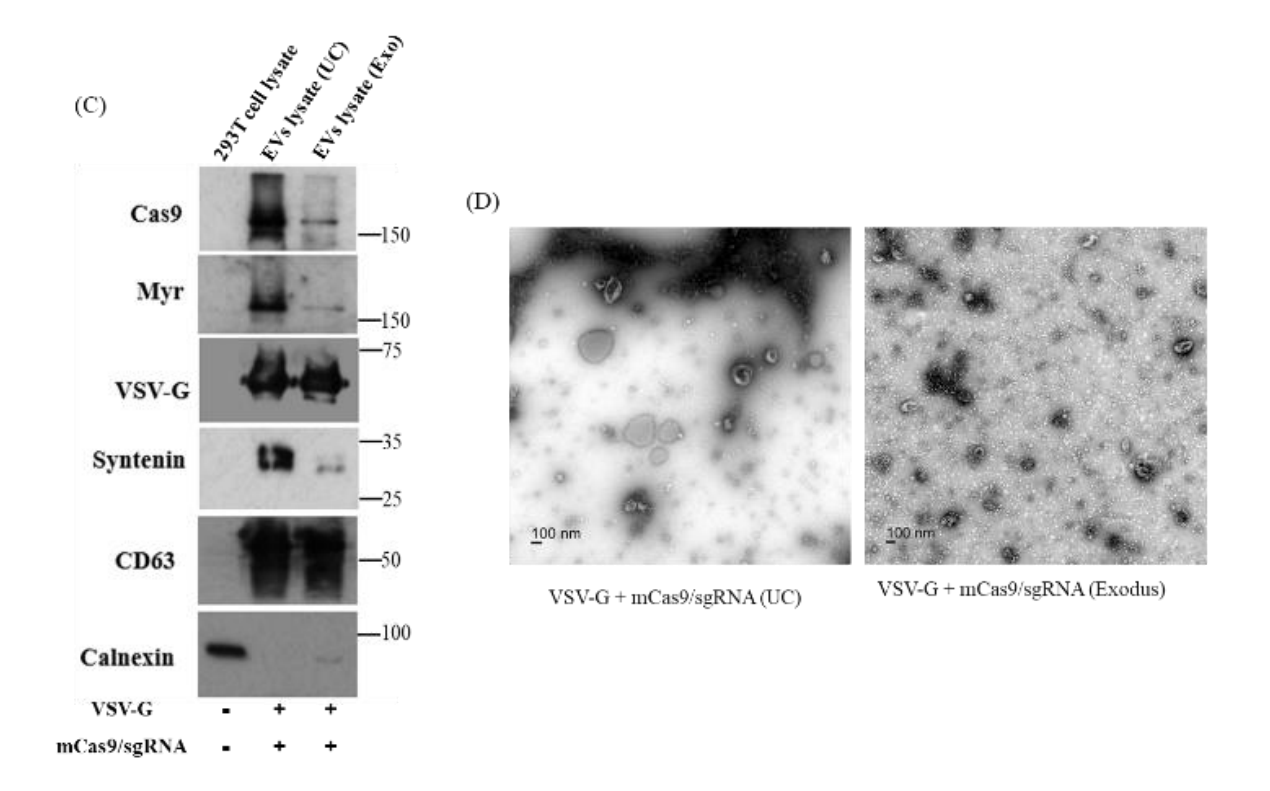


Figure 5 Production and characterization of EVs coated with VSV-G and encapsulating mCas9/sgRNA.

(A) Experimental schematic for producing EVs enveloped with VSV-G and encapsulating mCas9/sgRNA. HEK293T cells were co-transfected with 10 μg of VSV-G plasmid with/without 50 μg of mCas9/sgRNA plasmid in a 15cm-diameter plate. EVs from the transfected cells were harvested from the conditioned medium three days' post-transfection by ultracentrifugation or the Exodus machine. The transfected cells were expected to produce EVs expressing VSV-G with/without encapsulating mCas9/sgRNA. (B) The size distribution and concentration (particle number/mL) of EVs were measured using NanoSight Pro machine. The median diameter of EVs in the VSV-G group (n=6) and VSV-G + mCas9/sgRNA group (EVs encapsulating mCas9/sgRNA and expressing VSV-G, n=9) was determined. (C) EV lysates isolated from ultracentrifugation or the Exodus machine were subjected to Western blot analysis. Expression levels of Cas9, myristoylated Cas9, VSVG, syntenin and CD63 (the positive EVs protein biomarkers), and

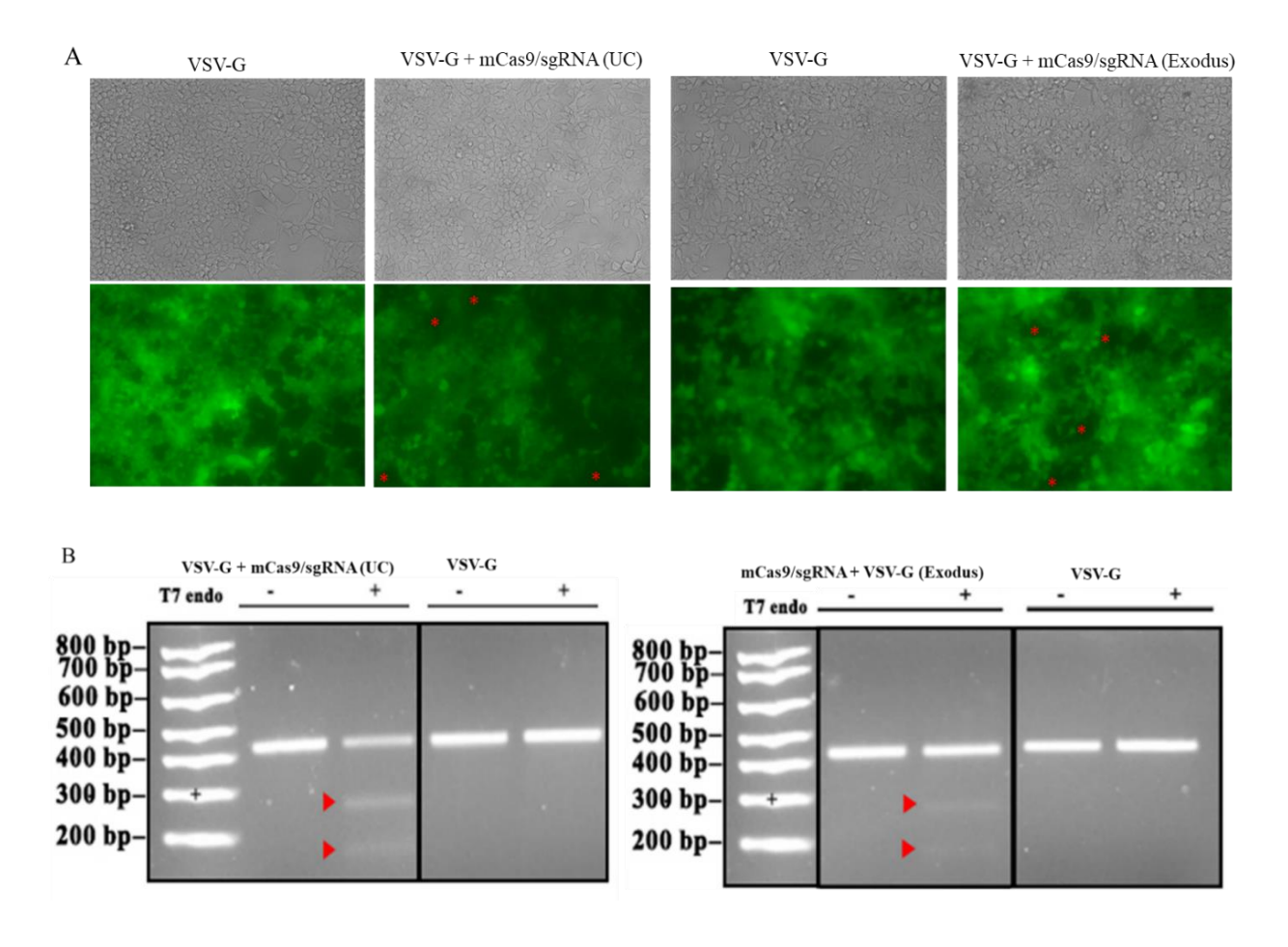
calnexin (a negative EVs protein biomarker) were determined. The protein lysate from 293T cells was served as a control. (D) The isolated EVs were subject to TEM analysis.

3. EVs Coated with VSV-G and Encapsulating mCas9/sgRNA Knocked out the eGFP Gene in HEK293T-eGFP Cells

We investigated the ability of the EVs coated with VSV-G and encapsulating mCas9/sgRNA targeting eGFP, isolated using both ultracentrifugation (UC) and the Exodus machine, could mediate gene editing in recipient cells. HEK293T-eGFP cells were subsequently treated with the EVs obtained from both isolation approaches as previously described. After treatment, we assessed the reduction in eGFP fluorescence in the recipient cells as an indicator of gene editing by the delivered EVs. A clear loss of green fluorescence was observed under fluorescence microscopy in cells treated with concentrated EVs coated by VSV-G and encapsulating mCas9/sgRNA from both isolation methods (Figure 6A). In contrast, recipient cells treated with EVs containing only VSV-G, without the CRISPR components, showed no evident of loss of eGFP expression, indicating that the observed gene knockout was specifically mediated by the CRISPR/Cas9 RNPs (Figure 6A). To further verify Cas9-mediated genome editing, a T7 endonuclease I (T7E1) mismatch assay was conducted. DNA cleavage within the sgRNA-eGFP target region was detected only in cells treated with CRISPR-loaded EVs, while no cleavage was observed in the control groups (Figure 6B).

To support these findings at the molecular level, we performed Sanger sequencing across three independent experiments, which revealed insertion-deletion (INDEL) mutations at the Cas9 target site in all treated groups. Specifically, HEK293T-eGFP cells treated with EVs isolated by UC showed the gene editing efficiency of 20% and 7%, respectively, while 13% of gene editing efficiency was detected in cells treated with EVs from the Exodus system (Figure 6C). Notably,

no INDELs were observed in the cells treated with VSV-G only EVs (Figure 6C). Taken together, these results confirm that VSV-G-enveloped EVs carrying CRISPR/Cas9 RNP complexes can effectively mediate precise and efficient gene editing in HEK293T-eGFP cells. Statistical analysis showed significantly higher editing in the EVs co-expressed VSV-G + mCas9/sgRNA group compared to the control ($p \le 0.05$).



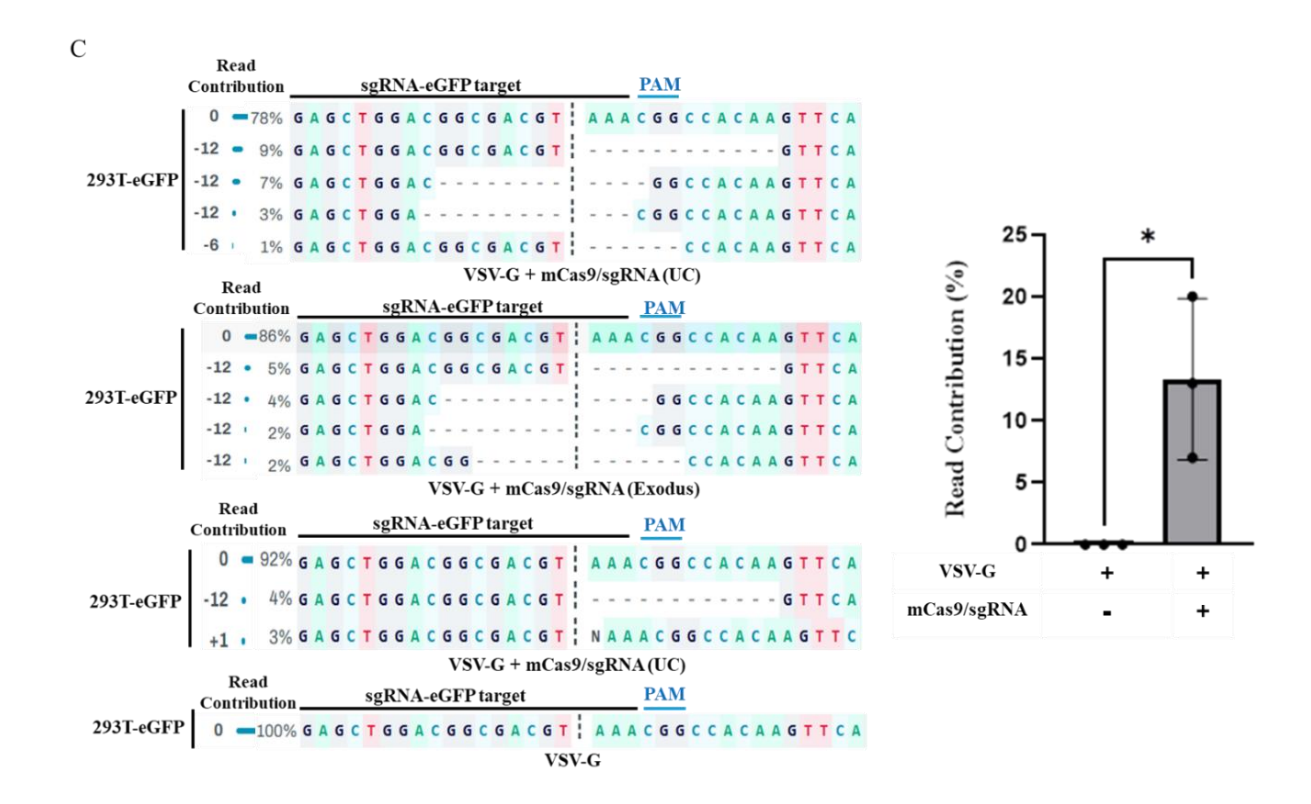


Figure 6 EVs encapsulating mCas9/sgRNA RNP complex coated with VSV-G mediated eGFP gene knockout in HEK293T-eGFP cells.

HEK293T-eGFP cells were treated twice, 48 hours apart, with EVs coated with VSV-G alone or with EVs co-expressing mCas9/sgRNA and VSV-G. After treatment, cells were evaluated for eGFP gene knockout. (A) The above treated cells were imaged by a fluorescent microscope to visualize eGFP expression. Cells treated with VSV-G + mCas9/sgRNA-eGFP EVs exhibited loss of green fluorescence, indicated by red asterisks, suggesting gene knockout. Cells treated with VSV-G-only EVs retained normal fluorescence, serving as a negative control. (B) A T7 endonuclease I (T7E1) mismatch cleavage assay was performed to validate genome editing. The PCR products were reannealed and digested with or without 10 U/μL T7E1 for 1 hour. If genome editing occurred, the PCR product should be digested into fragments as visualized on an agarose gel, and the cleaved bands were marked by red arrows. (C) Genomic DNA was extracted from the

treated cells and PCR was performed to amplify the sgRNA-eGFP target locus and was subjected to the Sanger sequencing from three independent experiments.

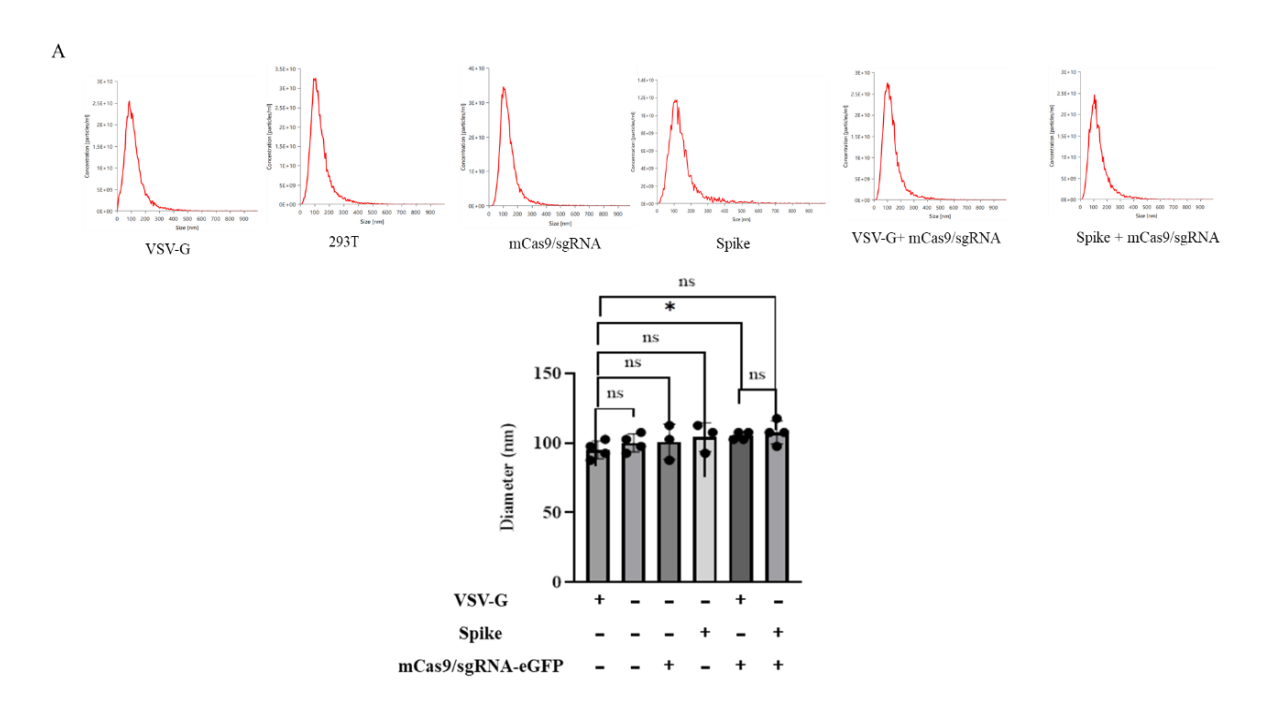
4. Spike Viral Protein Inhibited EVs Production and mCas9 Encapsulation Efficiency

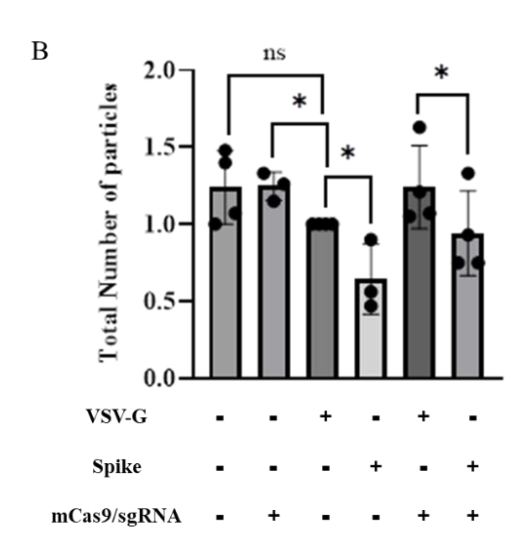
We compared the role of a mutated viral membrane spike protein (D614G-Δ21) (derived from SARS-CoV-2) and vesicular stomatitis virus glycoprotein (VSV-G) in EVs production and Cas9/sgRNA cargo-loading efficiency. HEK293T cells were transfected with/without vectors encoding VSV-G or spike(D614G-Δ21) and with/without mCas9/sgRNA. The average of the median diameter in control (293T without transfection), VSV-G, spike, mCas9/sgRNA, VSV-G + mCas9/sgRNA, and spike + mCas9/sgRNA groups was 100±6.45 nm, 95±6.45 nm, 104±10.41 nm, 101±12.58 nm, 105±2.89 nm, and 108±8.16 nm, respectively (Figure 7A). These data suggest that co-transfection with the CRISPR RNP components with/without viral protein did not affect the vesicle size.

To determine whether these viral proteins influence EVs production, we analyzed four independent batches of EVs. A significant reduction ($p \le 0.05$) in EVs production was observed in the spike-only group compared to the VSV-G control group (Figure 7B). Similarly, the total number of EVs in spike + mCas9/sgRNA group was also significantly lower than that in VSVG + mCas9/sgRNA group ($p \le 0.05$) (Figure 7B). The data suggest that the spike(D614G- Δ 21) protein may negatively impact EVs biogenesis.

Next, the detected expression of syntenin, CD9, and CD63, as well as the negative expression of calnexin in EVs suggested the quality of the concentrated EVs preparations (Figure 7C). As expected, the spike protein was detected in the EVs by the anti-S1 antibody and anti-S2 antibody in spike group and spike + mCas9/sgRNA. We next examined whether Cas9 protein enrichment in EVs was also observed when the spike viral protein was co-expressed. The expression levels of

Cas9 and mCas9 were significantly higher in the VSVG + mCas9/sgRNA group than those in spike + mCas9/sgRNA group, suggesting that spike protein is not favorable for the encapsulation of mCas9 into EVs (Figure 7C). Interestingly, myristoylated Src kinase levels were also inhibited in the spike + mCas9/sgRNA group. The total protein transferred to the membrane in western blotting was visualized using Ponceau S staining. Similar amount of protein was observed in all groups containing the EVs lysate (Figure 7C). Together, the data suggest that spike protein might inhibit EVs biogenesis, thereby influencing the myristoylated protein including Src and mCas9 being expressed in the EVs.





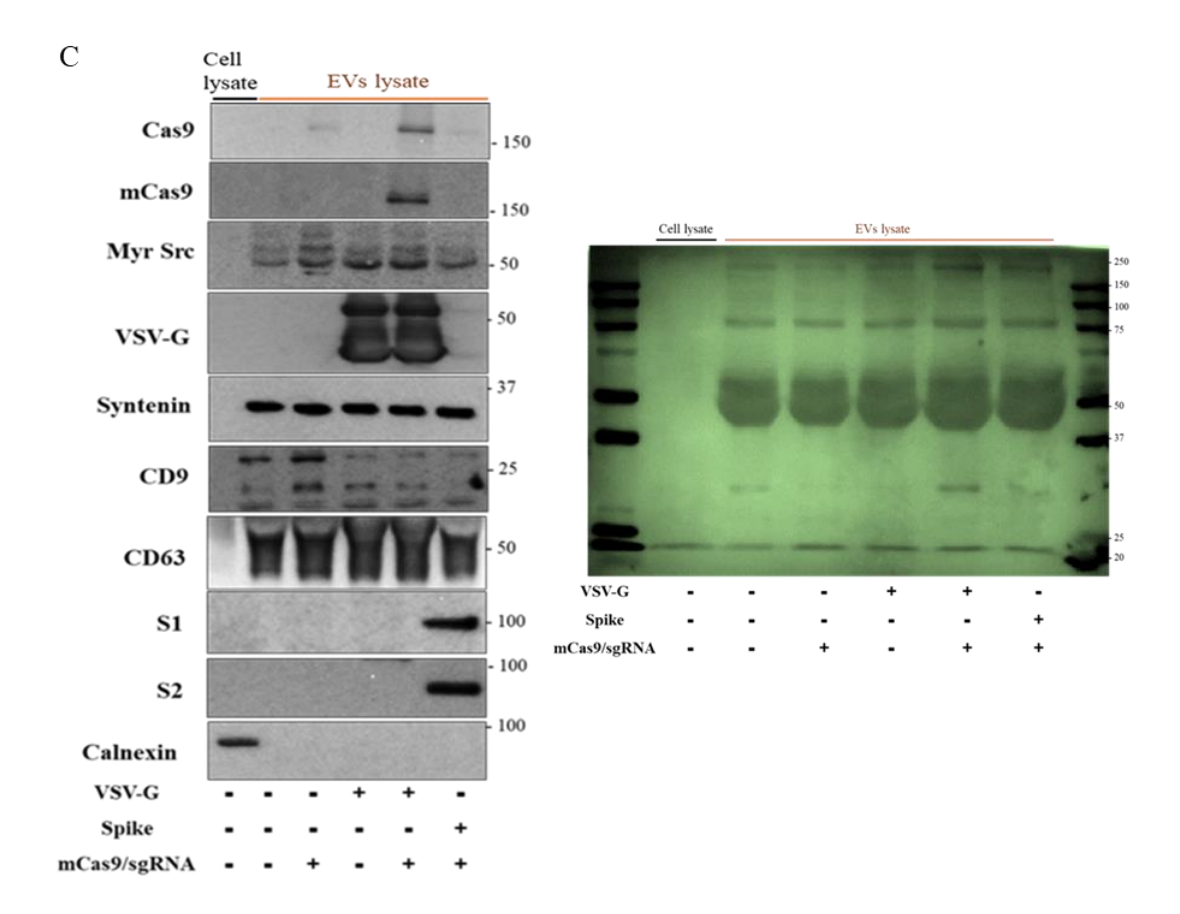


Figure 7 Spike(D614G- Δ 21) viral membrane protein inhibited EVs production and mCas9 encapsulation efficiency compared to VSV-G.

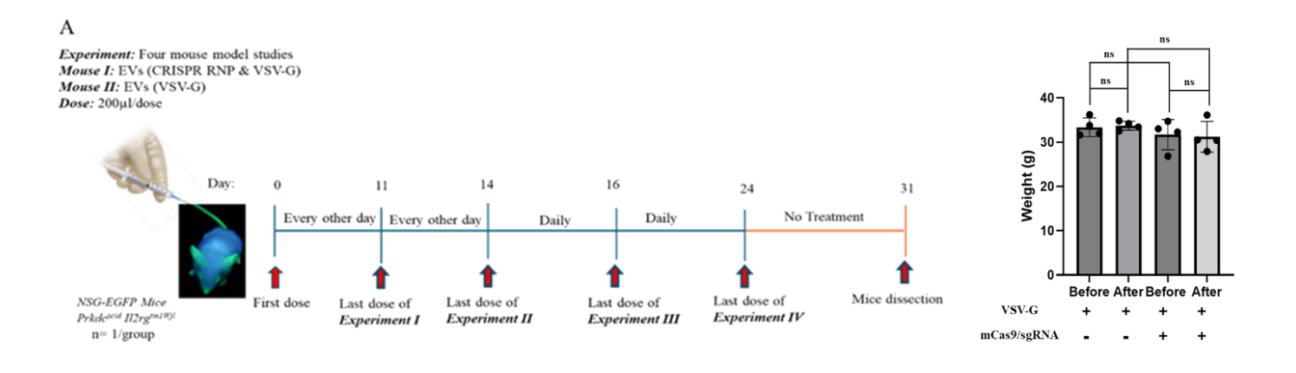
(A) HEK293T cells were transfected with/without VSV-G or spike(D614G- Δ 21) and with/without mCas9/sgRNA. The size distribution of EVs isolated from the above was measured

by NanoSight Pro., and the average of the was compared. (B) Total EVs numbers isolated from the conditioned medium were calculated based on the particle concentration measured by NanoSight. The total EVs number of the particles from VSV-G-only group were set as 1. Four independent experiments were conducted. (C) Expression levels of positive EVs protein biomarkers (syntenin, CD9, CD63), negative EVs protein biomarker (calnexin), Cas9, myristoylated Cas9 (mCas9), myristoylated Src, Src, VSVG, and viral envelope proteins (S1 and S2) in the EVs lysates were analyzed by Western blot. 293T cell lysate was served as a negative control. Western blot membranes were stained with Ponceau S to visualize the total protein transferred to the membrane.

5. In Vivo Evaluation of Endogenous eGFP Gene Editing in Various Organs Using EVs Encapsulating mCas9/sgRNA RNPs in NOD-SCID-EGFP Mouse Models

To explore the therapeutic potential of EVs-based delivery of CRISPR/Cas9 components for *in vivo* genome editing, we used an immunodeficient transgenic mouse model (NOD-SCID-EGFP) expressing enhanced green fluorescent protein (eGFP). The mice were administered EVs encapsulating mCas9/sgRNA-eGFP RNPs and coated with the fusogenic protein VSV-G to evaluate eGFP gene disruption in both systemic organs and tumor tissues (Figure 8A). We monitored body weight changes in all NOD-SCID-EGFP mice throughout the *in vivo* experiments. There was no significant weight loss or gain by comparing those before and after treatment (p>0.05) (Figure 8B). This observation suggests that repeated systemic administration of EVs, regardless of CRISPR cargo loading, was well tolerated by the animals, as weight loss is often used as a surrogate marker for systemic toxicity. The weight variation analysis supports that VSV-G-coated EVs serve as a non-toxic and safe delivery platform for CRISPR RNPs *in vivo*.

The mice were intravenously injected with CRISPR-loaded EVs to target the eGFP gene in various organs. The liver and lung tissues in Experiment 4 were subjected to both Sanger sequencing and Next Generation Sequencing (NGS) analysis (Figure 8C). Sanger sequencing results revealed no detectable INDELs in either the control or treatment groups in the analyzed experiment (Figure 8C, upper panel). This indicates that the editing efficiency was below the sensitivity threshold of the Sanger sequencing method. The experiment was further analyzed by Next Generation Sequencing, a more sensitive technique capable of identifying low-frequency mutations. 2% INDEL was detected in the targeted EGFP gene editing locus, corresponding to the sgRNA sequence, in the lung tissue of the treatment group (Figure 8C, lower panel). This low editing efficiency observed in systemic organs may reflect several biological barriers inherent to *in vivo* CRISPR delivery, including low EVs uptake by target cells, limited biodistribution, and inefficient nuclear delivery of the CRISPR RNPs. Nonetheless, the detection of editing through NGS confirms that the system is biologically active *in vivo*.



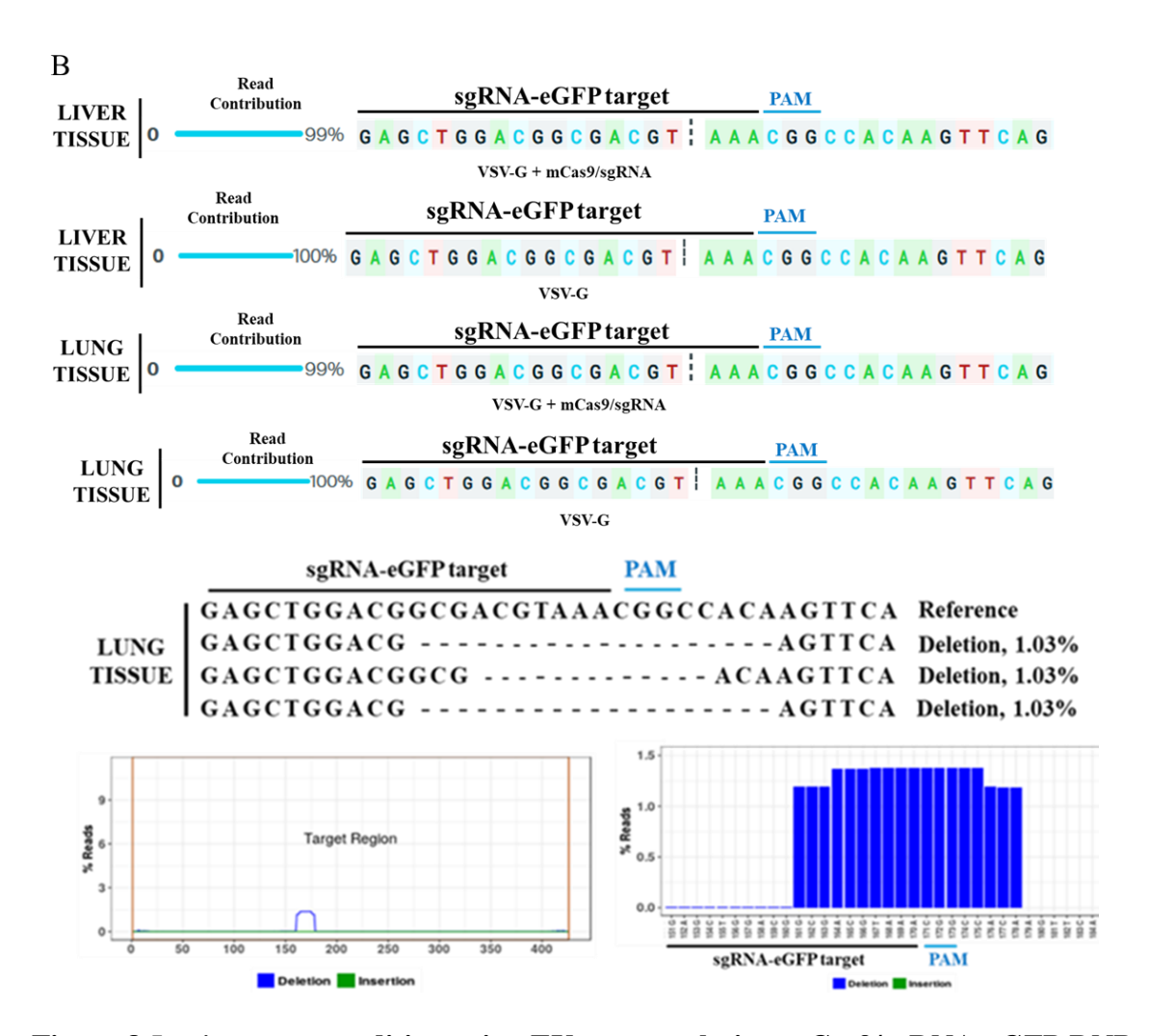


Figure 8 *In vivo* genome editing using EVs encapsulating mCas9/sgRNA-eGFP RNPs and coated with VSV-G in NSG-EGFP mouse models.

(A) Schematic representation of the *in vivo* experimental design. The *in vivo* study is comprised of four independent experiments to target endogenous eGFP gene in various organs. SCID mice were intravenously injected with EVs encapsulating mCas9/sgRNA-eGFP RNPs and coated with VSV-G (treatment) or EVs coated with VSV-G alone (control) to evaluate genome editing in targeting eGFP gene in various organs. In Experiment 1, six doses (200 μL/dose/mouse) were injected into the SCID-eGFP mouse by every other day. The total treatment was 11 days before the mouse was sacrificed. In Experiment 2, seven doses (200 μL/dose/mouse) were injected into

the SCID-eGFP mouse by every other day. The total treatment was 14 days before the mouse was sacrificed. In Experiment 3, sixteen doses (200 µL/dose/mouse, 4.20×10¹¹/mL) were injected into the SCID-eGFP mouse daily. The total treatment was 16 days before the mouse was sacrificed. In Experiment 4, twenty-four doses (200 µL/dose/mouse, 8.46×10¹¹/mL) were injected into the SCID-eGFP mouse daily. The total treatment was 24 days before the mouse was sacrificed. (B) The change of the body weight of SCID mice was monitored before and after EVs treatment. (C) Genome editing analysis of EGFP INDEL in lung and liver tissues was conducted in Experiment 4. The target region of EGFP was PCR-amplified and subjected to Sanger sequencing (upper panel) and Next Generation Sequencing (NGS) (lower panel).

6. In Vivo Evaluation of eGFP Gene Editing in Xenograft Tissues Using EVs Encapsulating mCas9/sgRNA RNPs in NOD-SCID-EGFP Mouse Models

We investigated the gene editing effect of EVs encapsulated mCas9/sgRNA-eGFP RNP in xenograft tissues expressing eGFP gene in SCID mice. The xenografts were established using either 293T-eGFP or C4-2B-eGFP cells. The EVs were intravenously injected to the mice to target the eGFP gene in xenograft tissues (Figure 9A). The xenograft tissues were collected and subjected to genomic analysis as described. Sanger sequencing did not detect any INDELs in the tissues from either the control or treatment groups (Figure 9B, upper panel). However, 1% INDEL was detected by Next Generation Sequencing at the targeted EGFP gene editing locus, corresponding to the sgRNA sequence, in both xenograft tissues of the treatment group (Figure 9B, lower panel), indicating low but measurable CRISPR-mediated disruption of the eGFP gene in xenograft tissues. Although the editing efficiency was exceedingly low, at only 1%, the fact that any editing was observed demonstrates proof of concept that EVs can function as delivery vehicles for genome-

editing cargos in xenograft tissues, highlighting the need for remarkable optimization for future gene therapy applications.

A Experiment: One mouse model study Subcutaneous Tumor Implantation: 1×106 293T-eGFP and C4-2B-eGFP cells Mouse I: EVs (mCas9/sgRNA-eGFP & VSV-G) Mouse II: EVs (VSV-G) Dose: 200µl/dose 38 0 Day: 30 Tumor Growth Daily SC injection 293T- & C4-Last dose Tumor NSG-EGFP Mice 2B -eGFP cells and C4-2B Mice dissection Appeared $Prkdc^{scid}\ Il2rg^{tm1Wjl}$ & C4-2B AR resistant cells n= 1/group

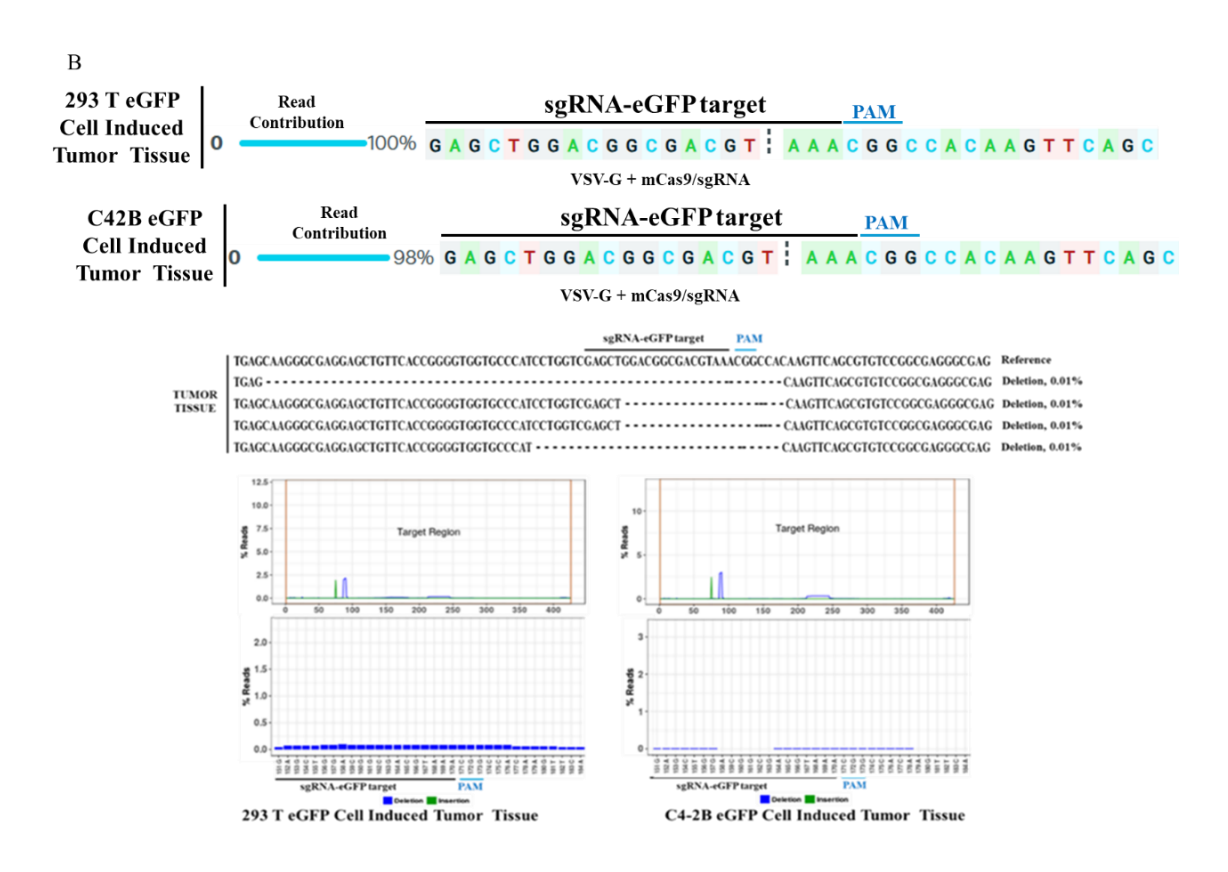


Figure 9 *In vivo* genome editing in xenograft tissues using EVs encapsulating mCas9/sgRNA-eGFP RNPs and coated with VSV-G in SCID mouse model.

(A) Schematic representation of the *in vivo* xenograft experimental design. The xenograft *in vivo* study is comprised of one independent experiment to target eGFP gene in xenograft tissues. SCID mice were intravenously injected with EVs encapsulating mCas9/sgRNA-eGFP RNPs and coated with VSV-G (treatment) or EVs coated with VSV-G alone (control) to evaluate genome editing in targeting eGFP gene in xenograft tissues. Eight doses (200 μL/dose/mouse, 1.40×10¹¹/mL) were injected into the xenograft SCID mouse daily. The total treatment was 08 days before the mouse was sacrificed. (B) Genome editing analysis of EGFP INDEL in xenograft tissues was conducted. The target region of EGFP was PCR-amplified and subjected to Sanger sequencing (upper panel) and Next Generation Sequencing (NGS) (lower panel).

CHAPTER 4

DISCUSSION

The CRISPR/Cas9 system represents a highly promising RNA-guided genome editing platform capable of precise DNA targeting. While various delivery methods have been explored, including physical techniques, viral vectors such as lentiviruses or adeno-associated viruses (AAV), and non-viral carriers like lipid-based systems and nanoparticles³, these approaches still face considerable limitations. Major challenges stem from the large molecular size of the CRISPR/Cas9 components (around 160 kDa), the distinct surface charges of Cas9 and single guide RNA (sgRNA), difficulties in encapsulation, the potential for triggering immune responses in the host, and the instability of the Cas9/sgRNA ribonucleoprotein (RNP) complex in circulation¹²⁰. EVs offer an attractive alternative due to their innate capacity to transport diverse biomolecules, low immunogenicity, and natural targeting ability. Their diagnostic and therapeutic value is further enhanced by their ability to carry cell-specific cargo, circulate widely through biological fluids, and elicit minimal immune reactions¹²¹.

In this study, we investigated EVs as a delivery vehicle for CRISPR/Cas9 machinery aimed at editing the eGFP gene in both *in vitro* and *in vivo* models. We also compared VSVG and the spike protein as functional moieties to enhance EV-mediated CRISPR RNP delivery. Our findings prove that EV-based delivery of CRISPR/Cas9 can knock out the eGFP gene *in vitro* and *in vivo*. Additionally, we demonstrate that spike protein inhibits EVs biogenesis and reduces its encapsulation efficiency of Cas9 compared to the VSV-G.

1. CRISPR/Cas9-Mediated Gene Editing Efficiency in HEK293T-eGFP Cells

The in vitro experiment to validate the effectiveness of the CRISPR/Cas9 system demonstrated that plasmid-encoded Cas9 and sgRNA targeting the eGFP gene achieved substantial gene editing in transfected HEK293T-eGFP cells. The results are consistent with earlier studies indicating that plasmid-based delivery allows for extended Cas9 and sgRNA expression, which facilitates efficient genome modification^{19,44}. Mechanistically, the sgRNA guides the Cas9 protein to the target DNA site via complementary base pairing between its 5' CRISPR RNA (crRNA) sequence and the genomic target. Cas9 then identifies a protospacer adjacent motif (PAM), specifically the 5'-NGG-3' sequence, where "N" represents any nucleotide. Upon PAM recognition, Cas9 induces a double-strand break (DSB) at the target locus 122. Our Sanger sequencing data further confirm this principle by revealing the introduction of site-specific mutations within the eGFP gene following CRISPR treatment (Figure 1C). Although plasmid-based delivery offers a straightforward and effective strategy for demonstrating proof-of-concept genome editing, it also presents inherent limitations. The sustained expression of Cas9 from plasmid DNA can prolong nuclease activity, increasing the risk of off-target DNA cleavage¹²³. Persistent Cas9 activity has been associated with activation of DNA damage response pathways and cellular toxicity, raising safety concerns for therapeutic applications. To address these issues, alternative delivery approaches such as direct delivery of ribonucleoprotein (RNP) complexes or Cas9 mRNA have gained attention.

2. Production and Characterization of VSV-G Coated EVs Encapsulating mCas9/sgRNA

In our study, we utilized EVs as a vehicle for delivering Cas9 ribonucleoprotein (RNP) complexes.

The EVs were modified with the viral envelope protein VSV-G to enhance cellular uptake and

improve EVs-mediated fusion with recipient cell membranes. Nanoparticle tracking analysis TEM images revealed that the VSV-G enveloped EVs maintained a uniform size and cup-shaped morphology, typically ranging from 105.8±8.66 nm to 109.2±6.06 nm in diameter, regardless of VSV-G modification or Cas9 cargo loading. Notably, EVs isolated by ultracentrifugation (UC) demonstrated higher levels of syntenin, Cas9, and N-myristoylated Cas9 compared to those isolated using the Exodus system. This is likely due to the EVs preparation isolated using the Exodus system retaining other proteins, most probably from the FBS containing medium used to suspend the EVs from the Exodus filter. These residual proteins may hinder proper lysis of the EVs, thereby limiting exposure of their internal materials. A key strategy in our study involved the use of N-myristoylation of Cas9 (mCas9) that enhances Cas9's association with membrane compartments, leading to more stable RNP formation within EVs¹¹⁷.

3. Genome Editing Activity of EVs-Delivered CRISPR RNPs in HEK293T-eGFP Cells We investigated the gene-editing efficiency of the EVs encapsulated mCas9/sgRNA and coated with VSV-G by treating HEK293T-eGFP cells targeting eGFP gene. Following EVs treatment, expected gene editing was observed in recipient HEK293T-eGFP cells. The ultracentrifugation (UC) isolated EVs achieved a higher gene editing efficiency (22%) compared to Exodus-isolated EVs, which reached only 14%. Our data also demonstrate that EVs isolated using the Exodus system expressed lower levels of Cas9 and mCas9 than those isolated by UC. This may be due to residual particles or proteins from the suspension medium used in the Exodus machine, which might interfere with the proper release of EVs cargo. This observation is further supported by TEM analysis, although EVs isolated by both methods show cup-shaped morphology, UC isolated EVs appear clearer, whereas Exodus isolated EVs are surrounded by and aggregated with other particles. However, these findings highlight the importance of EVs isolation techniques in

achieving functional delivery and biological efficacy of EVs preparations. This is because different isolation methods produce EVs with varying degrees of purity, integrity, cargo content, and size uniformity and all of which directly influence their uptake by recipient cells and their ability to deliver bioactive molecules such as proteins, RNAs, or CRISPR/Cas9 complexes^{124–126}.

In terms of the utilization of EVs as a vehicle to deliver Cas9/sgRNA RNP, the data in this study are consistent with previous reports that the VSVG-mediated delivery of Cas9/sgRNA RNP leads to the knock out of the eGFP gene in recipient cells^{117,127}. The editing efficiency, although lower than plasmid-based transfection, is promising given the biological complexity of RNP delivery and the transient nature of EVs-RNP complexes. Limited editing may be attributed to challenges such as endosomal entrapment, inefficient nuclear translocation of the RNP, and dilution during cell division.

4. Spike(D614G-Δ21) Inhibits the EVs Biogenesis and Cas9 Encapsulation Efficiency Compared with VSV-G

A comparative study was conducted to explore insight into optimizing EVs-based delivery systems with viral proteins, including spike protein and VSV-G for more effective and targeted gene therapy applications.

Virus membrane proteins have been integrated into the EVs as selective moieties to improve the delivery of various therapeutic cargos, including the Cas9/sgRNA RNP. VSV-G is one of the most commonly used as EVs enveloped protein. This VSV-G protein is particularly advantageous for gene therapy applications for its ability to facilitate endosomal escape after endocytosis¹²⁸, overcoming a major barrier in intracellular delivery of macromolecules. The ability of the SARS-CoV-2 spike protein to selectively target pulmonary epithelial cells¹²⁹ offers its potential the possibility for expanding the list of viral membrane proteins that can be repurposed for targeted

EVs delivery. The spike protein facilitates viral entry to the host cells by selectively binding to the ACE2 receptor^{130,131}.

However, our experimental data clearly demonstrate that the spike protein significantly ($p \le 0.05$) inhibits the generation of total EVs compared to VSV-G. As expected, the VSV-G co-expressed group showed a significant ($p \le 0.05$) increase in both EVs production and the encapsulation efficiency of CRISPR/Cas9 RNP complexes compared to the Spike (D614G-Δ21) co-expressed group. Moreover, VSV-G has been associated with increased levels of established EVs biomarker, including CD63 and CD9, as well as enhanced encapsulation of myristoylated Cas9, which may be due to its role in facilitating EVs biogenesis, including microvesicle formation through budding from the plasma membrane. Mechanistically, VSV-G is efficiently transported to the plasma membrane, where it supports vesicle formation by inducing membrane curvature and recruiting the ESCRT (endosomal sorting complexes required for transport) machinery^{132,133}. This process enables the efficient incorporation of protein cargos into EVs. In contrast, the spike protein may not engage these cellular mechanisms as effectively, which could explain its lower performance in facilitating EVs generation and cargo loading. Our data show a decrease of EVs numbers in the spike-transduced group, suggesting that the spike protein might inhibit the EVs biogenesis in the 293T cells. This result is consistent with the report by Cummings et al. 134, which demonstrated that expression of the wild-type SARS-CoV-2 Spike protein significantly reduced CD63 and CD9 levels in EVs derived from the transfected 293T, as shown by both flow cytometry and Western blot analyses, while the median diameter of EVs did not change. However, we did not observe significant decrease of CD63 or CD9 levels in EVs of the Spike mutant group by Western blot. It is unclear that the inconsistency was due to the spike wild type in their study versus the spike

mutant in ours. The comparison between the wild type spike and the spike mutant in the EVs biogenesis should be further carried out to resolve the inconsistency.

Interestingly, levels of myristoylated Src, a membrane-associated tyrosine kinase that plays a role in vesicle trafficking and membrane remodeling, were lower in the spike group. This reduction may reflect impaired vesicle formation or altered signaling pathways triggered by spike expression. Collectively, these findings suggest that while the spike protein incorporation may interfere with EVs biogenesis, VSV-G facilitates both vesicle formation and the efficient encapsulation of therapeutic cargos, thereby the therapeutic utility of EVs-based CRISPR delivery systems.

5. Systemic Delivery of CRISPR RNP Loaded EVs Demonstrates *In Vivo* Genome Editing

NOD.SCID-EGFP mice served as a model in our *in vivo* study to assess whether systemically administered CRISPR-loaded EVs could effectively deliver CRISPR/Cas9 ribonucleoprotein complexes into target tissues and facilitate gene editing. This approach allowed us to examine genome-editing efficiency of EVs-mediated CRISPR delivery *in vivo*.

No observable body weight loss was recorded throughout the course of the study, even after repeated intravenous administrations of CRISPR-loaded EVs. This absence of physiological abnormalities suggests that the EVs formulations used were well tolerated *in vivo* and do not elicit systemic toxicity, even with repeated dosing conditions. These findings provide important evidence supporting the biocompatibility of EVs as a safe vehicle for delivering genome-editing tools. Such outcomes support the ongoing development of EVs as a safe carrier for delivering genome-editing agents like CRISPR/Cas9 in clinical settings.

Liver and lung tissues were selected for DNA sequencing to evaluate *in vivo* gene editing efficiency following systemic administration of CRISPR-loaded EVs. These organs were chosen based on their known role as primary accumulation sites for systemically delivered nanoparticles, including EVs following intravenous administration and are well tolerated *in vivo* without inducing toxicity or organ damage^{135–137}. Therefore, analyzing these tissues provides for a reliable assessment to evaluate the *in vivo* gene-editing activity mediated by CRISPR RNPs delivered through EVs.

Sanger sequencing of liver and lung tissue samples did not reveal detectable INDELs (insertions or deletions) at the targeted genomic loci (eGFP). This result implies that either the EVs-delivered CRISPR RNPs failed to induce gene editing at the target site, or that CRISPR-mediated genome modifications occurred at frequencies too low for detection by Sanger sequencing. Sanger sequencing has a comparatively low sensitivity for detecting rare editing events, particularly in heterogeneous tissue samples where edited cells represent only a small proportion of the total population, including tumor and organ tissues^{138–140}. Therefore, the absence of visible INDELs in the sequencing chromatograms does not necessarily imply that editing did not occur, but rather that the frequency of edited alleles might be too low for reliable detection using this method. This limitation is particularly relevant in *in vivo* experiments where delivery efficiency, cellular uptake of CRISPR components, and editing activity may vary significantly between tissues and among individual cells.

While Sanger sequencing fails to detect any insertion or deletion (INDEL) mutations in liver and lung tissues, Next Generation Sequencing (NGS) offers for a much higher sensitivity and was able to detect low-frequency genome editing events. This makes it particularly well-suited for quantifying genome editing in heterogeneous tissues where only a small subset of cells may have

undergone successful CRISPR-mediated modifications. Using NGS, low-frequency INDELs were identified in both lung tissues (2%) and xenograft tissues (1%) following systemic administration of CRISPR-loaded EVs. These findings suggest that the CRISPR/Cas9 RNPs encapsulated within EVs were able to reach the target tissues, enter cells, and induce genome modifications, although the overall editing rates were modest. Importantly, the presence of INDELs in both normal and tumor tissues highlights the versatility of EVs for delivering genome-editing tools across different tissue types through systemic routes.

These low editing efficiencies reflect several known challenges associated with *in vivo* EVs-based delivery. The delivery efficiency of EVs *in vivo* is inherently limited due to physiological barriers. After intravenous injection, a significant portion of EVs is rapidly cleared by the reticuloendothelial system, primarily in the liver and spleen, which limits the availability of EVs in peripheral tissues such as the lungs^{141–143}. Moreover, effective delivery requires EVs to cross the vascular endothelium, navigate through tissue barriers, avoid nonspecific uptake, and successfully fuse with target cells to release their cargo into the appropriate intracellular compartment for gene editing to occur. These hurdles reduce the number of target cells that receive a sufficient dose of functional CRISPR/Cas9 ribonucleoprotein complexes^{144,145}. Furthermore, within tissues such as the lung and xenograft, cellular uptake of EVs can vary significantly across different cell types^{146,147}. Heterogeneity in receptor expression, endocytic pathways, and intracellular trafficking mechanisms influences whether CRISPR components reach the nucleus and induce genome editing.

Despite these obstacles, the detection of editing through NGS confirms that systemically delivered EVs can achieve functional gene editing *in vivo*. Although the editing frequencies were low, these results validate the potential of EVs as a delivery system for genome-editing applications.

Continued efforts to enhance EVs targeting specificity, optimize cargo loading, and improve dosing strategies will be essential to increase editing efficiency and fully realize the therapeutic potential of this delivery system.

Systemically delivered EVs may not accumulate efficiently at the target site due to rapid circulation clearance, biodistribution limitations, or lysosomal degradation or endosomal trap that may limit the delivery of Cas9 RNPs to the nucleus^{148–150}. Despite these challenges, this study is among the few to demonstrate *in vivo* gene editing using non-viral EVs-encapsulated Cas9 RNPs.

CHAPTER 5

LIMITATIONS AND FUTURE DIRECTIONS

Although this study highlights the promise of VSV-G enveloped EVs as a non-viral delivery system for CRISPR/Cas9-based gene editing, several limitations must be addressed before this platform can be translated into clinical applications. One of the key challenges is the natural heterogeneity of EVs populations and the inconsistent loading of therapeutic cargo, which can affect reproducibility and overall efficiency. Future approaches may benefit from the use of engineered EVs with improved control over cargo encapsulation and uniformity to enhance delivery consistency.

Another crucial area for development is the ability to direct EVs to specific tissues. In the current study, EVs were systemically administered, and although gene editing was detected in certain tissues, the delivery remained nonspecific. Incorporating targeting elements and utilizing real-time imaging with labeled EVs could refine dosing strategies and offer deeper insights into their pharmacokinetics and biodistribution *in vivo*.

Moreover, all *in vivo* experiments in this study were conducted in immunodeficient mouse models, which do not fully reflect the complexity of an intact immune system. Evaluating the performance of EVs-based CRISPR delivery in immunocompetent and tumor-bearing models will be essential to assess immune compatibility, off-target effects, and long-term safety. This will also provide critical insights into how the host environment influences EVs uptake, clearance, and genomeediting activity.

CHAPTER 6

CONCLUSION

Our findings present a strong proof-of-concept evidence supporting the use of VSV-G coated EVs as a non-viral carrier for delivering CRISPR/Cas9 RNPs. Through a combination of *in vitro* and *in vivo* models, we demonstrated that EVs can mediate functional genome editing to target the eGFP gene. *In vitro*, efficient knockout of eGFP confirmed the delivery and activity of the CRISPR/Cas9 system, while *in vivo* experiments showed functional but limited gene editing efficiency in lung and xenograft tissues. Notably, compared with VSV-G mediated gene editing, the spike (D614G-Δ21) protein significantly inhibited both the production of EVs and the encapsulation of Cas9 in EVs, which exhibited inferior performance. These results highlight the spike protein inhibits EVs biogenesis and cargo loading despite that spike protein has the specificity in targeting the ACE2 -expressing cells.

Although VSVG mediated gene editing efficiencies remained relatively low *in vivo*, this was expected given the biological complexity of systemic delivery and the known limitations of extracellular vesicles in crossing biological barriers, evading clearance, and targeting specific tissues. Still, the ability to observe gene editing in both normal and tumor tissues demonstrates that EVs can deliver functional CRISPR components to diverse *in vivo* environments. The study also reaffirmed the safety of EV-mediated delivery, with no signs of toxicity observed in treated animals. These findings align with previous research highlighting the biocompatibility and tolerability of EVs in systemic applications.

Overall, this study lays a strong background for the advancement of EV-based delivery systems for CRISPR/Cas9 therapeutics. With continued innovation in engineering and targeting, EVs-mediated gene editing holds significant promise for future clinical applications, particularly in treating genetic disorders and cancer.

REFERENCES

- 1. Jiang C, Meng L, Yang B, Luo X. Application of CRISPR/Cas9 gene editing technique in the study of cancer treatment. *Clin Genet*. 2020;97(1):73-88. doi:10.1111/cge.13589
- 2. Roth TL, Marson A. Genetic Disease and Therapy. *Annu Rev Pathol Mech Dis*. 2021;16(1):145-166. doi:10.1146/annurev-pathmechdis-012419-032626
- Ain QU, Chung JY, Kim YH. Current and future delivery systems for engineered nucleases:
 ZFN, TALEN and RGEN. J Control Release. 2015;205:120-127.
 doi:10.1016/j.jconrel.2014.12.036
- 4. Liang Y, Xu X, Xu L, et al. Chondrocyte-specific genomic editing enabled by hybrid exosomes for osteoarthritis treatment. *Theranostics*. 2022;12(11):4866-4878. doi:10.7150/thno.69368
- 5. Nassar W, El-Ansary M, Sabry D, et al. Umbilical cord mesenchymal stem cells derived extracellular vesicles can safely ameliorate the progression of chronic kidney diseases.

 *Biomater Res. 2016;20(1):21. doi:10.1186/s40824-016-0068-0
- 6. Bolotin A, Quinquis B, Sorokin A, Dusko Ehrlich S. Clustered regularly interspaced short palindrome repeats (CRISPRs) have spacers of extrachromosomal origin. *Microbiology*. 2005;151(8):2551-2561. doi:10.1099/mic.0.28048-0
- 7. Mojica FJM, Díez-Villaseñor C, García-Martínez J, Soria E. Intervening sequences of regularly spaced prokaryotic repeats derive from foreign genetic elements. *J Mol Evol*. 2005;60(2):174-182. doi:10.1007/s00239-004-0046-3
- 8. Ishino Y, Shinagawa H, Makino K, Amemura M, Nakatura A. Nucleotide sequence of the

- iap gene, responsible for alkaline phosphatase isoenzyme conversion in Escherichia coli, and identification of the gene product. *J Bacteriol*. 1987;169(12):5429-5433. doi:10.1128/jb.169.12.5429-5433.1987
- 9. Mojica FJM, Juez G, Rodriguez-Valera F. Transcription at different salinities of Haloferax mediterranei sequences adjacent to partially modified PstI sites. *Mol Microbiol*. 1993;9(3):613-621. doi:10.1111/j.1365-2958.1993.tb01721.x
- Jansen R, Van Embden JDA, Gaastra W, Schouls LM. Identification of genes that are associated with DNA repeats in prokaryotes. *Mol Microbiol*. 2002;43(6):1565-1575. doi:10.1046/j.1365-2958.2002.02839.x
- 11. Popkov VA, Zorova LD, Korvigo IO, et al. Do mitochondria have an immune system? Biochem. 2016;81(10):1229-1236. doi:10.1134/S0006297916100217
- 12. Pourcel C, Salvignol G, Vergnaud G. CRISPR elements in Yersinia pestis acquire new repeats by preferential uptake of bacteriophage DNA, and provide additional tools for evolutionary studies. *Microbiology*. 2005;151(3):653-663. doi:10.1099/mic.0.27437-0
- 13. Barrangou R, Marraffini LA. CRISPR-cas systems: Prokaryotes upgrade to adaptive immunity. *Mol Cell*. 2014;54(2):234-244. doi:10.1016/j.molcel.2014.03.011
- 14. Brouns SJJ, Jore MM, Lundgren M, et al. Small CRISPR RNAs guide antiviral defense in prokaryotes. *Science* (80-). 2008;321(5891):960-964. doi:10.1126/science.1159689
- 15. Deltcheva E, Chylinski K, Sharma CM, et al. CRISPR RNA maturation by trans-encoded small RNA and host factor RNase III. *Nature*. 2011;471(7340):602-607. doi:10.1038/nature09886
- 16. Jinek M, Chylinski K, Fonfara I, Hauer M, Doudna JA, Charpentier E. A programmable dual-RNA-guided DNA endonuclease in adaptive bacterial immunity. *Science* (80-).

- 2012;337(6096):816-821. doi:10.1126/science.1225829
- 17. Haft DH, Selengut J, Mongodin EF, Nelson KE. A guild of 45 CRISPR-associated (Cas) protein families and multiple CRISPR/cas subtypes exist in prokaryotic genomes. *PLoS Comput Biol.* 2005;1(6):0474-0483. doi:10.1371/journal.pcbi.0010060
- 18. Makarova KS, Haft DH, Barrangou R, et al. Evolution and classification of the CRISPR-Cas systems. *Nat Rev Microbiol*. 2011;9(6):467-477. doi:10.1038/nrmicro2577
- 19. Mali P, Yang L, Esvelt KM, et al. RNA-guided human genome engineering via Cas9. Science (80-). 2013;339(6121):823-826. doi:10.1126/science.1232033
- 20. Cong L, Ran FA, Cox D, et al. Multiplex genome engineering using CRISPR/Cas systems. Science (80-). 2013;339(6121):819-823. doi:10.1126/science.1231143
- 21. Mojica FJM, Rodriguez-Valera F. The discovery of CRISPR in archaea and bacteria. *FEBS J.* 2016;283(17):3162-3169. doi:10.1111/febs.13766
- 22. Marraffini LA. CRISPR-Cas immunity in prokaryotes. *Nature*. 2015;526(7571):55-61. doi:10.1038/nature15386
- 23. Heler R, Marraffini LA, Bikard D. Adapting to new threats: The generation of memory by CRISPR-Cas immune systems. *Mol Microbiol*. 2014;93(1):1-9. doi:10.1111/mmi.12640
- 24. Amitai G, Sorek R. CRISPR-Cas adaptation: Insights into the mechanism of action. *Nat Rev Microbiol*. 2016;14(2):67-76. doi:10.1038/nrmicro.2015.14
- Jiang F, Doudna JA. The structural biology of CRISPR-Cas systems. *Curr Opin Struct Biol*.
 2015;30:100-111. doi:10.1016/j.sbi.2015.02.002
- Van Der Oost J, Westra ER, Jackson RN, Wiedenheft B. Unravelling the structural and mechanistic basis of CRISPR-Cas systems. *Nat Rev Microbiol*. 2014;12(7):479-492. doi:10.1038/nrmicro3279

- 27. Wiedenheft B, Sternberg SH, Doudna JA. RNA-guided genetic silencing systems in bacteria and archaea. *Nature*. 2012;482(7385):331-338. doi:10.1038/nature10886
- 28. Gasiunas G, Barrangou R, Horvath P, Siksnys V. Cas9-crRNA ribonucleoprotein complex mediates specific DNA cleavage for adaptive immunity in bacteria. *Proc Natl Acad Sci U S A*. 2012;109(39). doi:10.1073/pnas.1208507109
- Mojica FJM, Díez-Villaseñor C, García-Martínez J, Almendros C. Short motif sequences determine the targets of the prokaryotic CRISPR defence system. *Microbiology*. 2009;155(3):733-740. doi:10.1099/mic.0.023960-0
- 30. Horvath P, Romero DA, Coûté-Monvoisin AC, et al. Diversity, activity, and evolution of CRISPR loci in Streptococcus thermophilus. *J Bacteriol*. 2008;190(4):1401-1412. doi:10.1128/JB.01415-07
- 31. Deveau H, Barrangou R, Garneau JE, et al. Phage response to CRISPR-encoded resistance in Streptococcus thermophilus. *J Bacteriol*. 2008;190(4):1390-1400. doi:10.1128/JB.01412-07
- 32. Doudna JA, Charpentier E. The new frontier of genome engineering with CRISPR-Cas9. Science (80-). 2014;346(6213). doi:10.1126/science.1258096
- 33. Meaker GA, Hair EJ, Gorochowski TE. Advances in engineering CRISPR-Cas9 as a molecular swiss army knife. *Synth Biol.* 2020;5(1). doi:10.1093/SYNBIO/YSAA021
- 34. Wright A V., Nuñez JK, Doudna JA. Biology and Applications of CRISPR Systems: Harnessing Nature's Toolbox for Genome Engineering. *Cell.* 2016;164(1-2):29-44. doi:10.1016/j.cell.2015.12.035
- 35. Lieber MR. The mechanism of double-strand DNA break repair by the nonhomologous DNA end-joining pathway. *Annu Rev Biochem*. 2010;79(1):181-211.

- doi:10.1146/annurev.biochem.052308.093131
- 36. San Filippo J, Sung P, Klein H. Mechanism of eukaryotic homologous recombination. *Annu Rev Biochem.* 2008;77(1):229-257. doi:10.1146/annurev.biochem.77.061306.125255
- 37. Garneau JE, Dupuis MÈ, Villion M, et al. The CRISPR/cas bacterial immune system cleaves bacteriophage and plasmid DNA. *Nature*. 2010;468(7320):67-71. doi:10.1038/nature09523
- 38. Horvath P, Barrangou R. CRISPR/Cas, the immune system of Bacteria and Archaea. Science (80-). 2010;327(5962):167-170. doi:10.1126/science.1179555
- 39. Pawelczak KS, Gavande NS, VanderVere-Carozza PS, Turchi JJ. Modulating DNA Repair Pathways to Improve Precision Genome Engineering. *ACS Chem Biol*. 2018;13(2):389-396. doi:10.1021/acschembio.7b00777
- 40. Alsaiari SK, Eshaghi B, Du B, et al. CRISPR–Cas9 delivery strategies for the modulation of immune and non-immune cells. *Nat Rev Mater*. 2024;10(1):44-61. doi:10.1038/s41578-024-00725-7
- 41. Lin Y, Wagner E, Lächelt U. Non-viral delivery of the CRISPR/Cas system: DNA versus RNA versus RNP. *Biomater Sci.* 2022;10(5):1166-1192. doi:10.1039/d1bm01658j
- 42. Fu Y, Foden JA, Khayter C, et al. High-frequency off-target mutagenesis induced by CRISPR-Cas nucleases in human cells. *Nat Biotechnol*. 2013;31(9):822-826. doi:10.1038/nbt.2623
- 43. Campbell LA, Coke LM, Richie CT, Fortuno L V., Park AY, Harvey BK. Gesicle-Mediated Delivery of CRISPR/Cas9 Ribonucleoprotein Complex for Inactivating the HIV Provirus.

 *Mol Ther. 2019;27(1):151-163. doi:10.1016/j.ymthe.2018.10.002
- 44. Kim S, Kim D, Cho SW, Kim J, Kim JS. Highly efficient RNA-guided genome editing in

- human cells via delivery of purified Cas9 ribonucleoproteins. *Genome Res*. 2014;24(6):1012-1019. doi:10.1101/gr.171322.113
- 45. Wang D, Zhang F, Gao G. CRISPR-Based Therapeutic Genome Editing: Strategies and In Vivo Delivery by AAV Vectors. *Cell*. 2020;181(1):136-150. doi:10.1016/j.cell.2020.03.023
- 46. Sonntag F, Schmidt K, Kleinschmidt JA. A viral assembly factor promotes AAV2 capsid formation in the nucleolus. *Proc Natl Acad Sci U S A*. 2010;107(22):10220-10225. doi:10.1073/pnas.1001673107
- 47. Lin SC, Haga K, Zeng XL, Estes MK. Generation of CRISPR–Cas9-mediated genetic knockout human intestinal tissue–derived enteroid lines by lentivirus transduction and single-cell cloning. *Nat Protoc*. 2022;17(4):1004-1027. doi:10.1038/s41596-021-00669-0
- 48. Behr M, Zhou J, Xu B, Zhang H. In vivo delivery of CRISPR-Cas9 therapeutics: Progress and challenges. *Acta Pharm Sin B*. 2021;11(8):2150-2171. doi:10.1016/j.apsb.2021.05.020
- 49. Lu CH, Chang YH, Lin SY, Li KC, Hu YC. Recent progresses in gene delivery-based bone tissue engineering. *Biotechnol Adv.* 2013;31(8):1695-1706. doi:10.1016/j.biotechadv.2013.08.015
- 50. Sung LY, Chen CL, Lin SY, et al. Enhanced and prolonged baculovirus-mediated expression by incorporating recombinase system and in cis elements: A comparative study. Nucleic Acids Res. 2013;41(14). doi:10.1093/nar/gkt442
- 51. Yin H, Kanasty RL, Eltoukhy AA, Vegas AJ, Dorkin JR, Anderson DG. Non-viral vectors for gene-based therapy. *Nat Rev Genet*. 2014;15(8):541-555. doi:10.1038/nrg3763
- 52. Lou D, Saltzman WM. Synthetic DNA delivery systems. *Nat Biotechnol*. 2000;18(1):33-37. doi:10.1038/71889

- 53. El Andaloussi S, Mäger I, Breakefield XO, Wood MJA. Extracellular vesicles: Biology and emerging therapeutic opportunities. *Nat Rev Drug Discov*. 2013;12(5):347-357. doi:10.1038/nrd3978
- 54. Yang B, Chen Y, Shi J. Exosome Biochemistry and Advanced Nanotechnology for Next-Generation Theranostic Platforms. *Adv Mater*. 2019;31(2):e1802896. doi:10.1002/adma.201802896
- 55. Lainšček D, Kadunc L, Keber MM, Bratkovič IH, Romih R, Jerala R. Delivery of an Artificial Transcription Regulator dCas9-VPR by Extracellular Vesicles for Therapeutic Gene Activation. *ACS Synth Biol.* 2018;7(12):2715-2725. doi:10.1021/acssynbio.8b00192
- 56. Peng J, Wang R, Sun W, et al. Delivery of miR-320a-3p by gold nanoparticles combined with photothermal therapy for directly targeting Sp1 in lung cancer. *Biomater Sci*. 2021;9(19):6528-6541. doi:10.1039/d1bm01124c
- 57. Luk BT, Zhang L. Cell membrane-camouflaged nanoparticles for drug delivery. *J Control Release*. 2015;220:600-607. doi:10.1016/j.jconrel.2015.07.019
- 58. Li T, Yang Y, Qi H, et al. CRISPR/Cas9 therapeutics: progress and prospects. *Signal Transduct Target Ther*. 2023;8(1):1-23. doi:10.1038/s41392-023-01309-7
- Yang HC, Chen PJ. The potential and challenges of CRISPR-Cas in eradication of hepatitis
 B virus covalently closed circular DNA. Virus Res. 2018;244:304-310.
 doi:10.1016/j.virusres.2017.06.010
- 60. Zischewski J, Fischer R, Bortesi L. Detection of on-target and off-target mutations generated by CRISPR/Cas9 and other sequence-specific nucleases. *Biotechnol Adv*. 2017;35(1):95-104. doi:10.1016/j.biotechadv.2016.12.003
- 61. Hsu PD, Lander ES, Zhang F. Development and applications of CRISPR-Cas9 for genome

- engineering. Cell. 2014;157(6):1262-1278. doi:10.1016/j.cell.2014.05.010
- 62. Senís E, Fatouros C, Große S, et al. CRISPR/Cas9-mediated genome engineering: An adeno-associated viral (AAV) vector toolbox. *Biotechnol J.* 2014;9(11):1402-1412. doi:10.1002/biot.201400046
- 63. White MK, Hu W, Khalili K. Gene Editing Approaches against Viral Infections and Strategy to Prevent Occurrence of Viral Escape. *PLoS Pathog*. 2016;12(12):e1005953. doi:10.1371/journal.ppat.1005953
- 64. Xu CL, Ruan MZC, Mahajan VB, Tsang SH. Viral delivery systems for crispr. *Viruses*. 2019;11(1):28. doi:10.3390/v11010028
- 65. Lee K, Conboy M, Park HM, et al. Nanoparticle delivery of Cas9 ribonucleoprotein and donor DNA in vivo induces homology-directed DNA repair. *Nat Biomed Eng*. 2017;1(11):889-901. doi:10.1038/s41551-017-0137-2
- 66. Mehravar M, Shirazi A, Nazari M, Banan M. Mosaicism in CRISPR/Cas9-mediated genome editing. *Dev Biol*. 2019;445(2):156-162. doi:10.1016/j.ydbio.2018.10.008
- 67. Chapman KM, Medrano GA, Jaichander P, et al. Targeted germline modifications in rats using CRISPR/Cas9 and spermatogonial stem cells. *Cell Rep.* 2015;10(11):1828-1835. doi:10.1016/j.celrep.2015.02.040
- 68. Li S. The basic characteristics of extracellular vesicles and their potential application in bone sarcomas. *J Nanobiotechnology*. 2021;19(1):1-12. doi:10.1186/s12951-021-01028-7
- 69. Skotland T, Sagini K, Sandvig K, Llorente A. An emerging focus on lipids in extracellular vesicles. *Adv Drug Deliv Rev.* 2020;159:308-321. doi:10.1016/j.addr.2020.03.002
- 70. Busatto S, Morad G, Guo P, Moses MA. The role of extracellular vesicles in the physiological and pathological regulation of the blood-brain barrier. *FASEB BioAdvances*.

- 2021;3(9):665-675. doi:10.1096/fba.2021-00045
- 71. Crescitelli R, Lässer C, Lötvall J. Isolation and characterization of extracellular vesicle subpopulations from tissues. *Nat Protoc*. 2021;16(3):1548-1580. doi:10.1038/s41596-020-00466-1
- 72. Han QF, Li WJ, Hu KS, et al. Exosome biogenesis: machinery, regulation, and therapeutic implications in cancer. *Mol Cancer*. 2022;21(1):1-26. doi:10.1186/s12943-022-01671-0
- 73. Lim HJ, Yoon H, Kim H, et al. Extracellular Vesicle Proteomes Shed Light on the Evolutionary, Interactive, and Functional Divergence of Their Biogenesis Mechanisms. Front Cell Dev Biol. 2021;9:734950. doi:10.3389/fcell.2021.734950
- 74. Perez-Hernandez D, Gutiérrez-Vázquez C, Jorge I, et al. The intracellular interactome of tetraspanin-enriched microdomains reveals their function as sorting machineries toward exosomes. *J Biol Chem.* 2013;288(17):11649-11661. doi:10.1074/jbc.M112.445304
- 75. Nagata S. Apoptosis and Clearance of Apoptotic Cells. *Annu Rev Immunol*. 2018;36(1):489-517. doi:10.1146/annurev-immunol-042617-053010
- 76. Zhang Y, Liu Y, Liu H, Tang WH. Exosomes: Biogenesis, biologic function and clinical potential. *Cell Biosci*. 2019;9(1):1-18. doi:10.1186/s13578-019-0282-2
- 77. Baietti MF, Zhang Z, Mortier E, et al. Syndecan-syntenin-ALIX regulates the biogenesis of exosomes. *Nat Cell Biol*. 2012;14(7):677-685. doi:10.1038/ncb2502
- 78. van Niel G, Charrin S, Simoes S, et al. The Tetraspanin CD63 Regulates ESCRT-Independent and -Dependent Endosomal Sorting during Melanogenesis. *Dev Cell*. 2011;21(4):708-721. doi:10.1016/j.devcel.2011.08.019
- 79. Gurung S, Perocheau D, Touramanidou L, Baruteau J. The exosome journey: from biogenesis to uptake and intracellular signalling. *Cell Commun Signal*. 2021;19(1):1-19.

- doi:10.1186/s12964-021-00730-1
- 80. Xie S, Zhang Q, Jiang L. Current Knowledge on Exosome Biogenesis, Cargo-Sorting Mechanism and Therapeutic Implications. *Membranes* (*Basel*). 2022;12(5):498. doi:10.3390/membranes12050498
- 81. Ghossoub R, Lembo F, Rubio A, et al. Syntenin-ALIX exosome biogenesis and budding into multivesicular bodies are controlled by ARF6 and PLD2. *Nat Commun*. 2014;5(1):1-12. doi:10.1038/ncomms4477
- 82. Meldolesi J. Extracellular vesicles (exosomes and ectosomes) play key roles in the pathology of brain diseases. *Mol Biomed*. 2021;2(1):18. doi:10.1186/s43556-021-00040-5
- 83. Kalra H, Drummen GPC, Mathivanan S. Focus on extracellular vesicles: Introducing the next small big thing. *Int J Mol Sci.* 2016;17(2):170. doi:10.3390/ijms17020170
- 84. Cocucci E, Meldolesi J. Ectosomes and exosomes: Shedding the confusion between extracellular vesicles. *Trends Cell Biol.* 2015;25(6):364-372. doi:10.1016/j.tcb.2015.01.004
- 85. Nabhan JF, Hu R, Oh RS, Cohen SN, Lu Q. Formation and release of arrestin domain-containing protein 1-mediated microvesicles (ARMMs) at plasma membrane by recruitment of TSG101 protein. *Proc Natl Acad Sci U S A*. 2012;109(11):4146-4151. doi:10.1073/pnas.1200448109
- 86. Sedgwick AE, Clancy JW, Olivia Balmert M, D'Souza-Schorey C. Extracellular microvesicles and invadopodia mediate non-overlapping modes of tumor cell invasion. *Sci Rep.* 2015;5(1):1-14. doi:10.1038/srep14748
- 87. Sun M, Xue X, Li L, et al. Ectosome biogenesis and release processes observed by using live-cell dynamic imaging in mammalian glial cells. *Quant Imaging Med Surg*. 2021;11(11):4604-4616. doi:10.21037/qims-20-1015

- 88. Gurunathan S, Kang MH, Qasim M, Khan K, Kim JH. Biogenesis, membrane trafficking, functions, and next generation nanotherapeutics medicine of extracellular vesicles. *Int J Nanomedicine*. 2021;16:3357-3383. doi:10.2147/JJN.S310357
- 89. Yu L, Zhu G, Zhang Z, et al. Apoptotic bodies: bioactive treasure left behind by the dying cells with robust diagnostic and therapeutic application potentials. *J Nanobiotechnology*. 2023;21(1):1-26. doi:10.1186/s12951-023-01969-1
- 90. Mohan A, Agarwal S, Clauss M, Britt NS, Dhillon NK. Extracellular vesicles: Novel communicators in lung diseases. *Respir Res.* 2020;21(1):175. doi:10.1186/s12931-020-01423-y
- 91. Santavanond JP, Rutter SF, Atkin-Smith GK, Poon IKH. Apoptotic Bodies: Mechanism of Formation, Isolation and Functional Relevance. In: *Subcellular Biochemistry*. Vol 97. La Trobe; 2021:61-88. doi:10.1007/978-3-030-67171-6_4
- 92. Zhang Q, Jeppesen DK, Higginbotham JN, et al. Supermeres are functional extracellular nanoparticles replete with disease biomarkers and therapeutic targets. *Nat Cell Biol*. 2021;23(12):1240-1254. doi:10.1038/s41556-021-00805-8
- 93. Yu J, Sane S, Kim JE, et al. Biogenesis and delivery of extracellular vesicles: harnessing the power of EVs for diagnostics and therapeutics. *Front Mol Biosci*. 2023;10:1330400. doi:10.3389/fmolb.2023.1330400
- 94. Mulcahy LA, Pink RC, Carter DRF. Routes and mechanisms of extracellular vesicle uptake. *J Extracell Vesicles*. 2014;3(1). doi:10.3402/jev.v3.24641
- 95. Morandi MI, Busko P, Ozer-Partuk E, et al. Extracellular vesicle fusion visualized by cryoelectron microscopy. *PNAS Nexus*. 2022;1(4):pgac156. doi:10.1093/pnasnexus/pgac156
- 96. Kaksonen M, Roux A. Mechanisms of clathrin-mediated endocytosis. *Nat Rev Mol Cell*

- Biol. 2018;19(5):313-326. doi:10.1038/nrm.2017.132
- 97. Mettlen M, Chen PH, Srinivasan S, Danuser G, Schmid SL. Regulation of Clathrin-Mediated Endocytosis. *Annu Rev Biochem*. 2018;87(Volume 87, 2018):871-896. doi:10.1146/annurev-biochem-062917-012644
- 98. Haddad D, Al Madhoun A, Nizam R, Al-Mulla F. Role of Caveolin-1 in Diabetes and Its Complications. *Oxid Med Cell Longev*. 2020;2020(1):9761539. doi:10.1155/2020/9761539
- 99. Gordon S. Phagocytosis: An Immunobiologic Process. *Immunity*. 2016;44(3):463-475. doi:10.1016/j.immuni.2016.02.026
- 100. Feng D, Zhao WL, Ye YY, et al. Cellular internalization of exosomes occurs through phagocytosis. *Traffic*. 2010;11(5):675-687. doi:10.1111/j.1600-0854.2010.01041.x
- 101. Czernek L, Chworos A, Duechler M. The Uptake of Extracellular Vesicles is Affected by the Differentiation Status of Myeloid Cells. *Scand J Immunol*. 2015;82(6):506-514. doi:10.1111/sji.12371
- 102. Fomina AF, Deerinck TJ, Ellisman MH, Cahalan MD. Regulation of membrane trafficking and subcellular organization of endocytic compartments revealed with FM1-43 in resting and activated human T cells. *Exp Cell Res.* 2003;291(1):150-166. doi:10.1016/S0014-4827(03)00372-0
- 103. Nabi IR, Le PU. Caveolae/raft-dependent endocytosis. *J Cell Biol*. 2003;161(4):673-677. doi:10.1083/jcb.200302028
- 104. Kamerkar S, Lebleu VS, Sugimoto H, et al. Exosomes facilitate therapeutic targeting of oncogenic KRAS in pancreatic cancer. *Nature*. 2017;546(7659):498-503. doi:10.1038/nature22341
- 105. Yang Z, Shi J, Xie J, et al. Large-scale generation of functional mRNA-encapsulating

- exosomes via cellular nanoporation. *Nat Biomed Eng.* 2020;4(1):69-83. doi:10.1038/s41551-019-0485-1
- 106. Vader P, Mol EA, Pasterkamp G, Schiffelers RM. Extracellular vesicles for drug delivery.

 *Adv Drug Deliv Rev. 2016;106(Pt A):148-156. doi:10.1016/j.addr.2016.02.006
- 107. Dooley K, McConnell RE, Xu K, et al. A versatile platform for generating engineered extracellular vesicles with defined therapeutic properties. *Mol Ther*. 2021;29(5):1729-1743. doi:10.1016/j.ymthe.2021.01.020
- 108. Gopalan D, Pandey A, Udupa N, Mutalik S. Receptor specific, stimuli responsive and subcellular targeted approaches for effective therapy of Alzheimer: Role of surface engineered nanocarriers. *J Control Release*. 2020;319:183-200. doi:10.1016/j.jconrel.2019.12.034
- 109. Xu X, Liang Y, Li X, et al. Exosome-mediated delivery of kartogenin for chondrogenesis of synovial fluid-derived mesenchymal stem cells and cartilage regeneration. *Biomaterials*. 2021;269:120539. doi:10.1016/j.biomaterials.2020.120539
- 110. Oliveira FD, Castanho MARB, Neves V. Exosomes and brain metastases: A review on their role and potential applications. *Int J Mol Sci.* 2021;22(19):10899. doi:10.3390/ijms221910899
- 111. Luo N, Li J, Chen Y, et al. Hepatic stellate cell reprogramming via exosome-mediated CRISPR/dCas9-VP64 delivery. *Drug Deliv*. 2021;28(1):10-18. doi:10.1080/10717544.2020.1850917
- 112. Lin Y, Wu J, Gu W, et al. Exosome–Liposome Hybrid Nanoparticles Deliver CRISPR/Cas9

 System in MSCs. *Adv Sci.* 2018;5(4):1700611. doi:10.1002/advs.201700611
- 113. Xu Q, Zhang Z, Zhao L, et al. Tropism-facilitated delivery of CRISPR/Cas9 system with

- chimeric antigen receptor-extracellular vesicles against B-cell malignancies. *J Control Release*. 2020;326:455-467. doi:10.1016/j.jconrel.2020.07.033
- 114. Chen C, Sun M, Wang J, Su L, Lin J, Yan X. Active cargo loading into extracellular vesicles: Highlights the heterogeneous encapsulation behaviour. *J Extracell Vesicles*. 2021;10(13):e12163. doi:10.1002/jev2.12163
- 115. McAndrews KM, Xiao F, Chronopoulos A, LeBleu VS, Kugeratski FG, Kalluri R. Exosome-mediated delivery of CRISPR/Cas9 for targeting of oncogenic KrasG12D in pancreatic cancer. *Life Sci Alliance*. 2021;4(9):e202000875. doi:10.26508/LSA.202000875
- 116. Zhuang J, Tan J, Wu C, et al. Extracellular vesicles engineered with valency-controlled DNA nanostructures deliver CRISPR/Cas9 system for gene therapy. *Nucleic Acids Res*. 2020;48(16):8870-8882. doi:10.1093/nar/gkaa683
- 117. Whitley JA, Kim S, Lou L, et al. Encapsulating Cas9 into extracellular vesicles by protein myristoylation. *J Extracell Vesicles*. 2022;11(4):e12196. doi:10.1002/jev2.12196
- 118. Wang C, Liu Z, Chen Z, et al. The establishment of reference sequence for SARS-CoV-2 and variation analysis. *J Med Virol*. 2020;92(6):667-674. doi:10.1002/jmv.25762
- 119. Crawford KHD, Eguia R, Dingens AS, et al. Protocol and reagents for pseudotyping lentiviral particles with SARS-CoV-2 spike protein for neutralization assays. *Viruses*. 2020;12(5):513. doi:10.3390/v12050513
- 120. Li L, Hu S, Chen X. Non-viral delivery systems for CRISPR/Cas9-based genome editing:
 Challenges and opportunities. *Biomaterials*. 2018;171:207-218.
 doi:10.1016/j.biomaterials.2018.04.031
- 121. Zhao Y, Li X, Zhang W, et al. Trends in the biological functions and medical applications of extracellular vesicles and analogues. *Acta Pharm Sin B*. 2021;11(8):2114-2135.

- doi:10.1016/j.apsb.2021.03.012
- 122. Ceasar SA, Rajan V, Prykhozhij S V., Berman JN, Ignacimuthu S. Insert, remove or replace:

 A highly advanced genome editing system using CRISPR/Cas9. *Biochim Biophys Acta Mol Cell Res*. 2016;1863(9):2333-2344. doi:10.1016/j.bbamcr.2016.06.009
- 123. Adli M. The CRISPR tool kit for genome editing and beyond. *Nat Commun*. 2018;9(1):1-13. doi:10.1038/s41467-018-04252-2
- 124. Kowal J, Arras G, Colombo M, et al. Proteomic comparison defines novel markers to characterize heterogeneous populations of extracellular vesicle subtypes. *Proc Natl Acad Sci U S A*. 2016;113(8):E968-E977. doi:10.1073/pnas.1521230113
- 125. Mateescu B, Kowal EJK, van Balkom BWM, et al. Obstacles and opportunities in the functional analysis of extracellular vesicle RNA An ISEV position paper. *J Extracell Vesicles*. 2017;6(1):1286095. doi:10.1080/20013078.2017.1286095
- 126. Li P, Kaslan M, Lee SH, Yao J, Gao Z. Progress in exosome isolation techniques. *Theranostics*. 2017;7(3):789-804. doi:10.7150/thno.18133
- 127. Whitley JA, Cai H. Engineering extracellular vesicles to deliver CRISPR ribonucleoprotein for gene editing. *J Extracell Vesicles*. 2023;12(9):e12343. doi:10.1002/jev2.12343
- 128. Ma D, Xie A, Lv J, et al. Engineered extracellular vesicles enable high-efficient delivery of intracellular therapeutic proteins. *Protein Cell*. 2024;15(10):724-743. doi:10.1093/procel/pwae015
- 129. Perico L, Morigi M, Pezzotta A, et al. SARS-CoV-2 spike protein induces lung endothelial cell dysfunction and thrombo-inflammation depending on the C3a/C3a receptor signalling. *Sci Rep.* 2023;13(1):1-12. doi:10.1038/s41598-023-38382-5
- 130. Wang Q, Zhang Y, Wu L, et al. Structural and Functional Basis of SARS-CoV-2 Entry by

- Using Human ACE2. Cell. 2020;181(4):894-904.e9. doi:10.1016/j.cell.2020.03.045
- 131. Koehler M, Delguste M, Sieben C, Gillet L, Alsteens D. Initial Step of Virus Entry: Virion Binding to Cell-Surface Glycans. *Annu Rev Virol*. 2020;7(1):143-165. doi:10.1146/annurev-virology-122019-070025
- 132. Robison CS, Whitt MA. The Membrane-Proximal Stem Region of Vesicular Stomatitis Virus G Protein Confers Efficient Virus Assembly. *J Virol.* 2000;74(5):2239-2246. doi:10.1128/jvi.74.5.2239-2246.2000
- 133. Balch WE, McCaffery JM, Plutner H, Farquhar MG. Vesicular stomatitis virus glycoprotein is sorted and concentrated during export from the endoplasmic reticulum. *Cell*. 1994;76(5):841-852. doi:10.1016/0092-8674(94)90359-X
- 134. Cummings SE, Delaney SP, St-Denis Bissonnette F, et al. SARS-CoV-2 antigen-carrying extracellular vesicles activate T cell responses in a human immunogenicity model. *iScience*. 2024;27(1):108708. doi:10.1016/j.isci.2023.108708
- 135. Lázaro-Ibánez E, Al-Jamal KT, Dekker N, et al. Selection of fluorescent, bioluminescent, and radioactive tracers to accurately reflect extracellular vesicle biodistribution in vivo. ACS Nano. 2021;15(2):3212-3227. doi:10.1021/acsnano.0c09873
- 136. Gangadaran P, Hong CM, Ahn BC. An update on in vivo imaging of extracellular vesicles as drug delivery vehicles. *Front Pharmacol*. 2018;9:169. doi:10.3389/fphar.2018.00169
- 137. Yi YW, Lee JH, Kim SY, et al. Advances in analysis of biodistribution of exosomes by molecular imaging. *Int J Mol Sci.* 2020;21(2):665. doi:10.3390/ijms21020665
- 138. Ishige T, Itoga S, Matsushita K. Locked Nucleic Acid Technology for Highly Sensitive Detection of Somatic Mutations in Cancer. In: *Advances in Clinical Chemistry*. Vol 83. Elsevier; 2018:53-72. doi:10.1016/bs.acc.2017.10.002

- 139. Herreros-Villanueva M, Chen CC, Yuan SSF, Liu TC, Er TK. KRAS mutations: Analytical considerations. *Clin Chim Acta*. 2014;431:211-220. doi:10.1016/J.CCA.2014.01.049
- 140. Shackelford RE, Whitling NA, McNab P, Japa S, Coppola D. KRAS Testing: A Tool for the Implementation of Personalized Medicine. *Genes and Cancer*. 2012;3(7-8):459-466. doi:10.1177/1947601912460547
- 141. Ohno SI, Takanashi M, Sudo K, et al. Systemically injected exosomes targeted to EGFR deliver antitumor microrna to breast cancer cells. *Mol Ther*. 2013;21(1):185-191. doi:10.1038/mt.2012.180
- 142. Bala S, Csak T, Momen-Heravi F, et al. Biodistribution and function of extracellular miRNA-155 in mice. *Sci Rep.* 2015;5(1):1-12. doi:10.1038/srep10721
- 143. Smyth T, Kullberg M, Malik N, Smith-Jones P, Graner MW, Anchordoquy TJ. Biodistribution and delivery efficiency of unmodified tumor-derived exosomes. *J Control Release*. 2015;199:145-155. doi:10.1016/j.jconrel.2014.12.013
- 144. Vader P, Mol EA, Pasterkamp G, Schiffelers RM. Extracellular vesicles for drug delivery.

 *Adv Drug Deliv Rev. 2016;106(Pt A):148-156. doi:10.1016/j.addr.2016.02.006
- 145. György B, Hung ME, Breakefield XO, Leonard JN. Therapeutic applications of extracellular vesicles: Clinical promise and open questions. *Annu Rev Pharmacol Toxicol*. 2015;55(1):439-464. doi:10.1146/annurev-pharmtox-010814-124630
- 146. Mulcahy LA, Pink RC, Carter DRF. Routes and mechanisms of extracellular vesicle uptake. *J Extracell Vesicles*. 2014;3(1):24641. doi:10.3402/jev.v3.24641
- 147. Ginini L, Billan S, Fridman E, Gil Z. Insight into Extracellular Vesicle-Cell Communication: From Cell Recognition to Intracellular Fate. *Cells*. 2022;11(9):1375. doi:10.3390/cells11091375

- 148. Lázaro-Ibánez E, Al-Jamal KT, Dekker N, et al. Selection of fluorescent, bioluminescent, and radioactive tracers to accurately reflect extracellular vesicle biodistribution in vivo. ACS Nano. 2021;15(2):3212-3227. doi:10.1021/acsnano.0c09873
- 149. Ribovski L, Joshi BS, Gao J, Zuhorn IS. Breaking free: endocytosis and endosomal escape of extracellular vesicles. *Extracell Vesicles Circ Nucleic Acids*. 2023;4(2):283-305. doi:10.20517/evcna.2023.26
- 150. Wan Z, Zhao L, Lu F, et al. Mononuclear phagocyte system blockade improves therapeutic exosome delivery to the myocardium. *Theranostics*. 2020;10(1):218-230. doi:10.7150/thno.38198